METHODOLOGY   **Open Access**

Quality assurance of 3D-printed patient specific anatomical models: a systematic review

Martin Schulze[1*†], Lukas Juergensen[1†], Robert Rischen[2], Max Toennemann[1], Gregor Reischle[3], Jan Puetzler[1], Georg Gosheger[1] and Julian Hasselmann[1,4]

Abstract

Background The responsible use of 3D-printing in medicine includes a context-based quality assurance. Considerable literature has been published in this field, yet the quality of assessment varies widely. The limited discriminatory power of some assessment methods challenges the comparison of results. The total error for patient specific anatomical models comprises relevant partial errors of the production process: *segmentation error (SegE)*, *digital editing error (DEE)*, *printing error (PrE)*. The present review provides an overview to improve the general understanding of the process specific errors, quantitative analysis, and standardized terminology.

Methods This review focuses on literature on quality assurance of patient-specific anatomical models in terms of geometric accuracy published before December 4th, 2022 ($n = 139$). In an attempt to organize the literature, the publications are assigned to comparable categories and the *absolute values of the maximum mean deviation (AMMD)* per publication are determined therein.

Results The three major examined types of *original structures* are teeth or jaw ($n = 52$), skull bones without jaw ($n = 17$) and heart with coronary arteries ($n = 16$). VPP (vat photopolymerization) is the most frequently employed basic 3D-printing technology ($n = 112$ experiments). The median values of *AMMD* (AMMD: The metric AMMD is defined as the largest linear deviation, based on an average value from at least two individual measurements.) are 0.8 mm for the *SegE*, 0.26 mm for the *PrE* and 0.825 mm for the total error. No average values are found for the *DEE*.

Conclusion The *total error* is not significantly higher than the *partial errors* which may compensate each other. Consequently *SegE, DEE* and *PrE* should be analyzed individually to describe the result quality as their sum according to rules of error propagation. Current methods for quality assurance of the segmentation are often either realistic and accurate or resource efficient. Future research should focus on implementing models for cost effective evaluations with high accuracy and realism. Our system of categorization may be enhancing the understanding of the overall process and a valuable contribution to the structural design and reporting of future experiments. It can be used to educate specialists for risk assessment and process validation within the additive manufacturing industry.

Keywords Anatomical models, Quality assurance, Medical additive manufacturing, 3D-printing, Segmentation error, Digital editing error, Printing error, Error classification

†Martin Schulze and Lukas Juergensen contributed equally to this work.

*Correspondence:
Martin Schulze
martin.schulze@ukmuenster.de
Full list of author information is available at the end of the article

Background

3D-printing in medicine

The technologies of 3D-printing in medicine have revolutionized patient care and treatment strategies. From fabricating patient-specific anatomical models [1, 2] to producing customized surgical guides [3, 4] and implants [5, 6], 3D-printing offers rapid, precise and tailored solutions that facilitate medical education [7, 8], improve patient information [9, 10] and enhance procedural and surgical outcomes [11, 12].

In the responsible use of 3D-printing in medicine, sufficient and context-based quality assurance must be guaranteed in terms of patient safety. This implies the need for a quality assurance program covering the entire production process and interfaces to adjacent processes. This essentially includes manufacturing tolerances, which certainly may vary depending on the subsequent use case of the 3D-print. Determining these can be done in a variety of ways and is not trivial. For a comparison with defined manufacturing tolerances, the error must be accurately assessed.

Quality assurance of 3D-printed patient specific anatomical models

The 3D Printing Special Interest Group of the Radiological Society of North America has already established guidelines for medical 3D-printing, which describe recommendations for quality assurance [13]. Although considerable literature has been published in this field, the methods used to assess quality vary widely. Due to the limited discriminatory power of some assessment methods the comparison of results between different authors is challenging. This aspect has already been discussed by Illi et al. [14] and Chae et al. [15].

The present review focuses on the literature on quality assurance of patient-specific anatomical models in terms of geometric accuracy published before December 4th, 2022. As an attempt to organize the literature, the included publications are assigned to comparable categories and the *absolute values of the maximum mean deviation* (AMMD) per publication are determined therein. The present review provides an overview from the perspective of the clinical user to improve the general understanding of the process specific errors. The goal is to facilitate access for future systematic approaches and reporting through suggested standardized terminology.

The medical 3D-printing process and its errors

The production of patient-specific anatomical models is a multi-step process, in which each individual step may involve a partial error.

The production process begins with imaging of the original structure, e.g. computed tomography from patients (clinical setting), cadaveric specimens, anatomical models or phantoms (experimental setting). The resulting data sets are stored in Digital Imaging and Communications in Medicine (DICOM) file format. A virtual three-dimensional model is generated from the DICOM data sets by segmentation. In most cases the standard tessellation language (STL) file format is used for saving a model. This format is a translation of the model into a three-dimensional mesh structure of triangles and normal vectors. These STLs are prone to errors such as artefacts, mesh gaps and misorientation of the normal vectors, but can be corrected by various, partly automated, partly manual repair methods including smoothing (digital editing). However, if the resolution of the mesh is low, the model may deviate significantly from the original (Fig. 1).

Digital editing techniques help to generate a print-STL file of good quality, which is translated into a machine-readable code (slicing). This code, which may be printer-specific, is then interpreted by the 3D-printer in order to build a 3D object layer by layer. After the built is completed, a material and printing technology-dependent post-processing is necessary, e.g. removal of support structures or a curing with ultraviolet light.

Figure 2 shows the process for the production of patient-specific 3D-printed anatomical models.

The ISO (International Organization for Standardization) 5725–2:2019 standard describes the accuracy of measurement methods in terms of *trueness* and *precision* [16]. In medical 3D-printing, those can be determined for each individual process step. *Trueness* is determined by calculating the error between the reference and the result of a single sub-step within the overall process. *Precision* is assessed by comparing multiple results of a single sub-step of the overall process when performed repeatedly [17, 18].

Materials and methods

Screening of the literature

A systematic literature search was conducted in Scopus and PubMed (Medline database) according to the Preferred Reporting Items for Systematic Reviews and Meta-Analyses (PRISMA) guidelines. The following search algorithms were used.

Scopus: TITLE-ABS-KEY ((accuracy OR ("quality control") OR ("quality assurance") OR assessment) AND ((models OR modeling) AND ("3D printing" OR "3D printed" OR "additive manufacturing")) AND NOT bioprinting).

Medline: (accuracy[Title/Abstract] OR ("quality control"[Title/Abstract]) OR ("quality assurance"[Title/Abstract]) OR assessment [Title/Abstract]) AND ((models[Title/Abstract] OR modeling[Title/Abstract]) AND ("3D printing"[Title/Abstract] OR "3D printed"[Title/
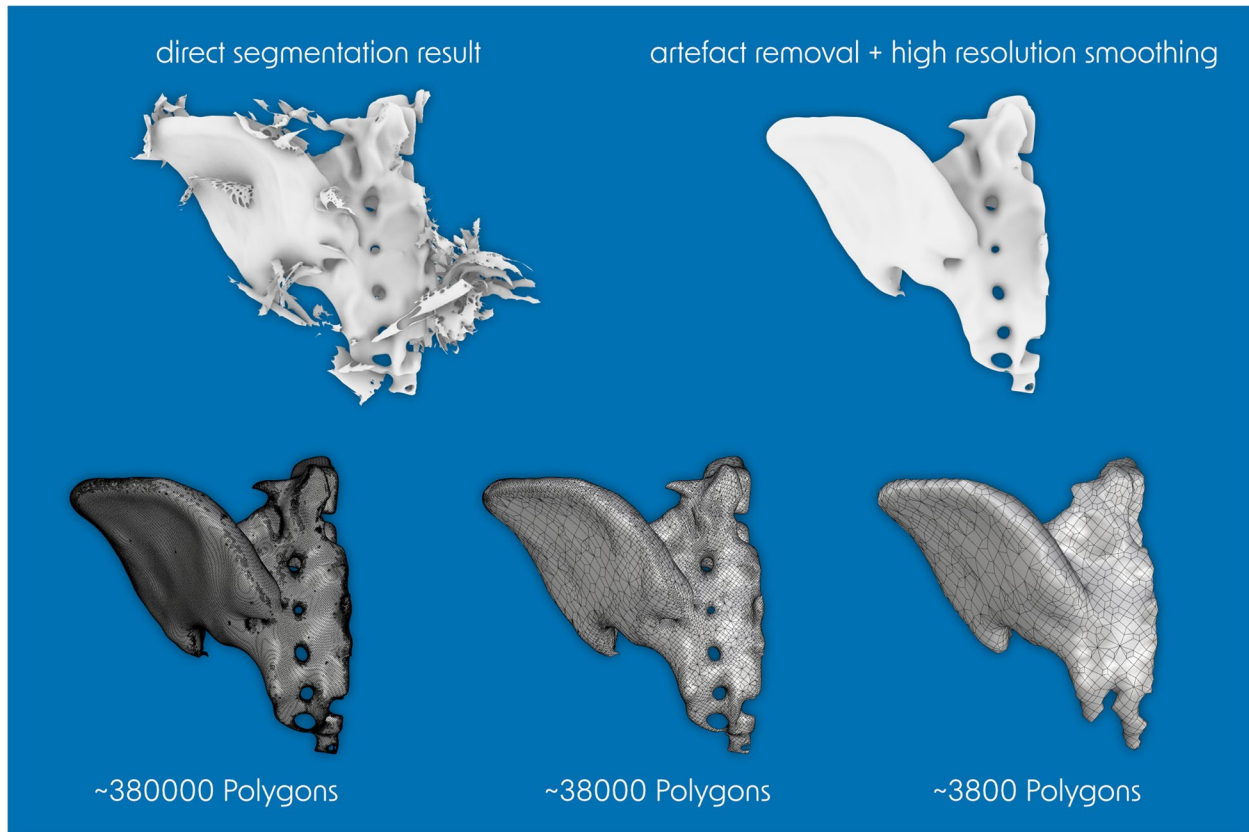
Fig. 1 Visualization of artefact removal, smoothing and reduction of mesh density with a loss of anatomical details. A left hemipelvis is shown as an example. When the number of polygons is reduced by a factor of 100, the anatomical details of the neuroforamina and sacral segments are lost
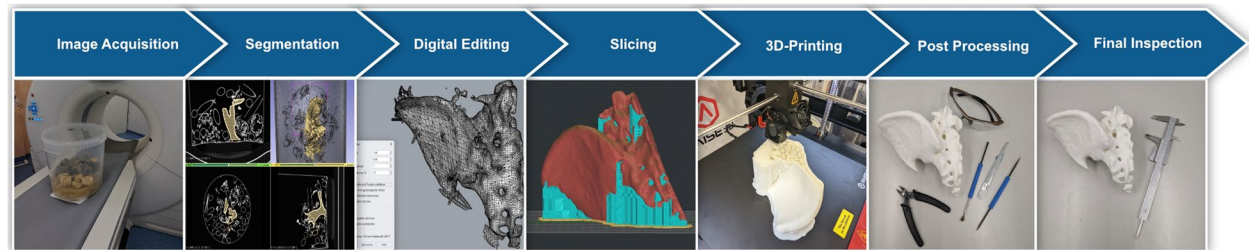

Fig. 2 Medical 3D-printing process for the production of patient specific anatomical models

Abstract] OR additive manufacturing [Title/Abstract])) NOT bioprinting [Title/Abstract].

The initial search on December 4th 2022 resulted in 5923 search results on Scopus and 1105 on PubMed, respectively. The results were exported using research information system format (RIS) and imported into Citavi (Swiss Academic Software GmbH, V6.1, Wädenswil, Switzerland) for deduplication. 1014 duplicate records in total were removed before screening. 6014 records were screened by title of which 5747 were

excluded manually due to exclusion criteria as shown in Table 1.

Categories for classifying measurements

When quantifying errors in the medical 3D-printing processes, it is important to consider which steps of the whole process are evaluated and how this evaluation takes place. One example for this is that the accuracy of the segmentation process is greatly influenced by whether adjacent tissue (simulated or real) is included in
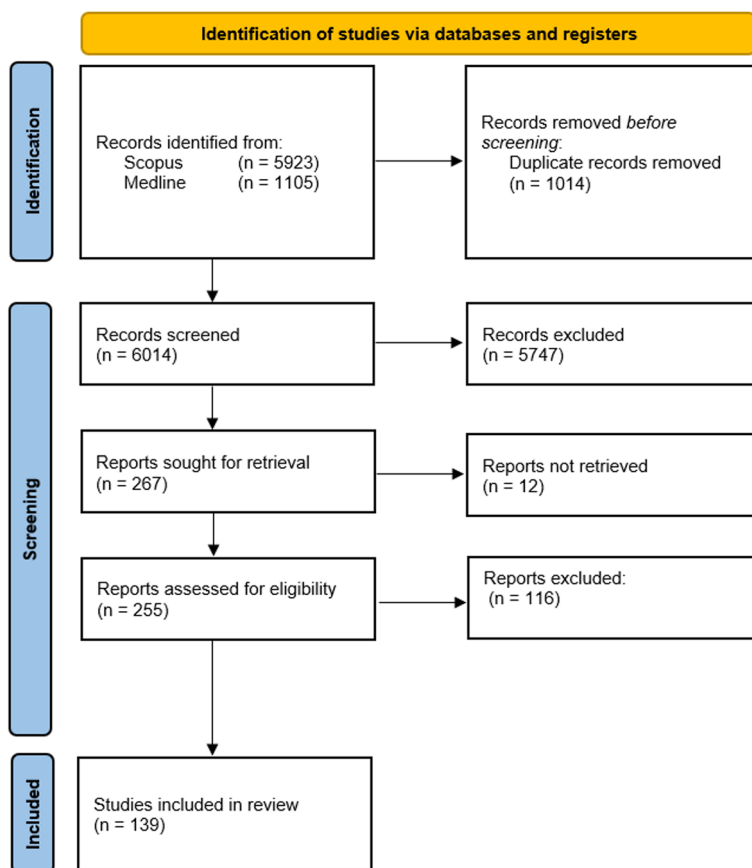
Fig. 3 PRISMA flow chart resulting in 139 articles included [66]

the image acquisition, or whether the *original structure* is scanned in air [67]. The following overview presents categories which contain comparable measurements from the literature.

Individual and combined errors in medical 3D-printing processes

Figure 4 shows the process for the production of patient-specific 3D-printed anatomical models, including the main types of errors that can occur. In addition to the process shown in Fig. 2, the intermediate results of each sub-step are also shown. Partial errors and their possible combinations are distinguished. The combined investigation of partial errors is possible if they refer to directly consecutive process steps. Thus, the combination of segmentation error (SegE) and digital editing error (DEE) can be examined as well as the combination of DEE and and printing error (PrE). The total error can be examined as a combination of SegE, DEE and PrE.

As *image acquisition* not only represents the initial step of the production process but also serves as a tool for measuring the *original structure*, a peculiarity arises for errors involving the SegE: there are two possible process

steps where reference measurements can be taken: a) directly on the original structure e.g. using a caliper or b) on the DICOM data using linear measurement tools. Assuming that *the image acquisition error* (IAE) is an externally controlled parameter to our model with tight error tolerances guaranteed by the specialized discipline of medical physics according to manufacturer specifications [68], in this publication, the term "*segmentation error*" refers not only to the individual *segmentation error* (SegE), but also to the combined error of *image acquisition* (IAE) and *segmentation* (IAE + SegE). Consequently, the individual IAE is not separately considered in the combined error analyses beyond the SegE.

In general, the focus is on the *trueness* of various steps involved in the process of creating patient-specific anatomical models. However, regarding the *segmentation error*, publications that evaluate *precision* are also included, as this step requires the most manual input.

In the following section, the main types of errors are defined and the methodology for categorizing experiments to evaluate medical 3D-printing processes is outlined. The categorization of the included literature is based on the methods for conducting measurements on

Table 1 In- and exclusion criteria for title screening

Inclusion Criteria	Example	Exclusion Criteria	Example
quality assessment of medical models	[19]	clinical studies	[20]
tolerances of additive manufactured objects for clinical use	[21]	no medical context	[22]
additive manufactured models in medicine	[23]	evaluation of material properties	[24]
improving accuracy of 3D-printing	[25]	usage of printed models for surgery simulation instead of cadavers	[26]
review 3D-printing in medicine	[27]	mechanical properties of parts produced with metal powder bed fusion	[28]
quality assessment of segmentation	[29]	effect on patient education	[30]
comparison of different printing processes	[31]	assessment of using 3D-printing for education of professionals	[8]
quality assessment of printing process	[32]	assessment of surgery results	[33]
review and validation	[14]	using 3D-printed models as phantoms for radiology, nuclear medicine or radio therapy	[34]
		using 3D-printing for mechanical analyses	[35]
		accuracy assessment of surgical guides	[36]
		general opportunities of 3D-printing in medicine	[37]
		planning and simulation of surgeries using 3D-printing	[38]
		analysis and prediction of printing quality from the perspective of engineers	[39]
		functional models	[40]
		analysis of energy consumption or cost	[41]
		biomedical implants	[42]
		only review	[43]
		general improvements of printing process from the perspective of engineers	[44]
		models that simulate haptic reality	[45]
		assessment of color	[46]
		review of 3D-printing for surgical teaching	[47]

Of the remaining 267 reports 12 were not retrieved (three because full texts were not accessible and nine because language was not English or German). Out of the remaining 255 reports, 116 were excluded after full text screening due to exclusion criteria as shown in Table 2. 139 Studies were included in this review (Fig. 3)

both the *original structures* and the *printed models,* as well as the experimental setup of the *image acquisition.* A visualization of the error subcategories is shown in Fig. 5 and a more detailed description of all subcategories can be found in Appendix A.

Evaluation of the segmentation error (SegE)

The SegE is defined as the deviation between the *original structure* and the direct result of the segmentation process. All experiments assessing SegE are further subdivided by the measurement methods used and the experimental setups of the image acquisition.

Evaluation of the digital editing error (DEE)

The DEE is defined as the deviation between the direct result of the segmentation process and the *print-STL.* All experiments assessing the DEE are further subdivided by whether a linear measurement-based or a surface deviation-based analysis was performed.

Evaluation of the printing error (PrE)

The PrE is defined as the deviation between the *print-STL* and the *printed model.* All experiments assessing the PrE are further subdivided by the measurement tools used.

Evaluation of the image acquisition error (IAE)

The IAE is defined as the deviation between the *original structure* and the result of the *image acquisition* (DICOM data set).

Evaluation of the segmentation comparison error (SegC)

The SegC is defined as the precision of the segmentation process when it is performed repeatedly, e.g. by different users or with different software.

Combination of segmentation error and digital editing error (SegE+DEE)

The combination of SegE and DEE is defined as the deviation between the *original structure* and the *print-STL.* All experiments assessing the combined error of SegE

Table 2 Exclusion criteria for full text screening with one example for each

Exclusion Criteria	Example
influences on the printing process from the engineers' perspective	[32]
influences of slicing tools on printing accuracy from the engineers' perspective	[48]
accuracy of implants	[49]
assessment of special post processing techniques like vapor smoothing	[50]
assessment of surface properties	[51]
assessment of STL-export from CAD software	[52]
evaluation of ageing process of printed models	[53]
evaluation of thermoformed appliances	[54]
using 3D-printed models for assessment of image acquisition	[55]
phantoms for MRI	[56]
evaluation of an experimental full-automatic segmentation algorithm	[57]
evaluation of 3D-printed models as diagnostic tool in comparison to the standard	[58]
accuracy assessment of 3D-printed surgical guides	[59]
realistic surgery models for procedure assessment	[60]
evaluation of 3D-printed models as a diagnostic tool in comparison to the standard	[58]
only visual evaluation	[61]
only review	[62]
only clinical study	[63]
only case report	[64]
no validation	[65]

and DEE are further subdivided by measurement methods and experimental setups of the *image acquisition*. For this purpose, the SegE subcategories are used.

Combination of digital editing error and printing error (DEE + PrE)

The combination of DEE and PrE is defined as the deviation between the direct result of the segmentation process and the *printed model*. All experiments assessing the combination of DEE and PrE are further subdivided by the measurement tools used. For this purpose, the PrE subcategories are used.

Combination of segmentation error, digital editing error and printing error (SegE+DEE + PrE)

The combination of SegE, DEE and PrE is defined as the deviation between the *original structure* and the *printed model*. All experiments assessing the *total error* are further subdivided by measurement methods and experimental setups of the *image acquisition*. For this purpose, combinations of SegE and PrE subcategories are used.

Subcategories for the detailed analysis of applied methods

Sections 2.2.2 to 2.2.9 defined the main error types describing which process steps of the medical 3D printing process are compared with each other. However, it should also be considered which methods are applied for this comparison, as they can differ significantly in their realism and accuracy. To describe the applied methods in detail, they were analyzed on four levels: 1. the basic approach, 2. the imaging setup, 3. the tools for linear measurements, and 4. the time of the dissection. Within the basic approach, a distinction is made between methods that apply linear measurements (lin), e.g. between two landmarks, and those that apply software-supported surface comparisons (surf). In the case of surface comparisons, for example, the resulting digital model from an optical 3D scan of an original structure could be compared with the direct segmentation result after an iterative alignment. The imaging setup, together with the timing of the dissection, is primarily responsible for the realism of an experiment. A distinction was made between artificial models scanned in air environment (nosim), artificial models scanned with simulation of adjacent tissue (sim), cadaver studies (cad) and real patients (pat). For linear measurement tools, calipers (cal), virtual software-supported calipers after a 3D scan was conducted (3Dcal), and CT combined with linear measurements on resulting DICOM data for measurements of printed models (DICOM) were distinguished. For cadaver studies, the realism of an experiment also depends on whether the dissection was done before imaging (dis) (e.g., scanning dry bones) or after imaging (nodis) (e.g., scanning wet specimens). Figure 5 shows a visualization of the subcategories for the main types of error, including the four levels for method analysis "basic approach", "imaging setup", "tools for linear measurements" and "time of dissection".

(See figure on next page.)

Fig. 4 Medical 3D-printing process for the production of patient specific anatomical models and its errors. In addition to the steps of the process shown in Fig. 2, the intermediate results are also shown. The arrows indicate which of the intermediate process results are compared to determine the respective main types of error, including the differentiation of *combined* and *partial errors*. Highlighted with blue box: Errors that should be evaluated individually according to the guidelines of the RSNA for medical 3D-printing [13]. SegE: *Segmentation Error*, DEE: *Digital Editing Error*, PrE: *Printing Error*, IAE: *Image Acquisition Error*, SegC: *Segmentation Comparison Error*. PrE: most frequently evaluated *partial error*, SegE+DEE + PrE: most frequently evaluated *combined error*
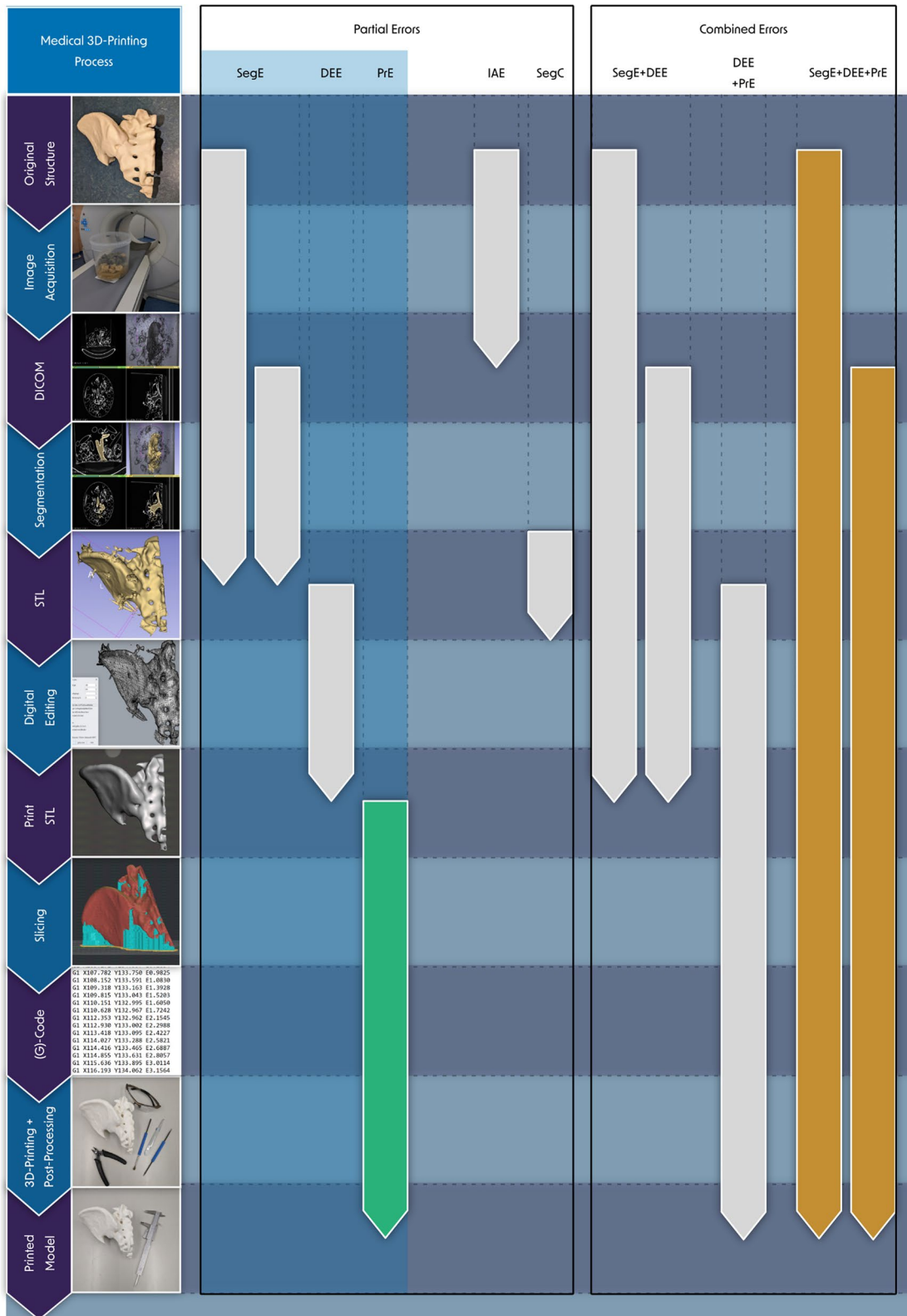
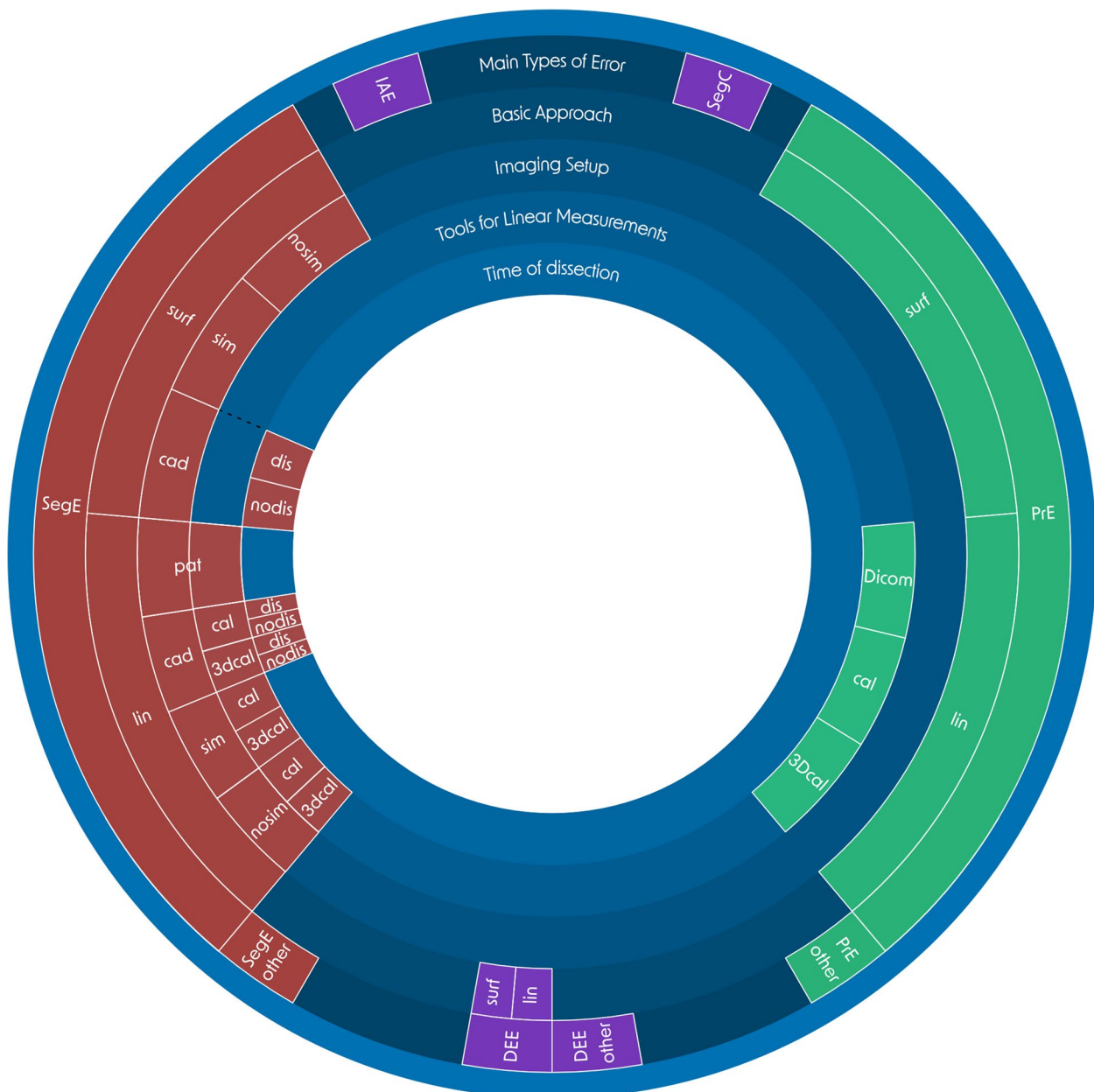**Fig. 4** (See legend on previous page.)

Fig. 5 Visualization of the subcategories for the detailed analysis of applied methods. *Main types of error*: IAE: *Image Acquisition Error*, SegE: *Segmentation Error*, SegC: *Segmentation Comparison Error*, DEE: *Digital Editing Error*, PrE: *Printing Error*; basic approach: linear (lin) or surface (surf) deviation based analysis; imaging setup: experimental setups of the image acqusition: nosim: artifical model and no simulation of adjacent tissue, sim: artifical model and simulation of adjacent tissue, cad: cadaver study, pat: scan of patients due to clinical questions; tools for linear measurements: DICOM: CT-Scan of 3D-printed model and linear measurements on resulting DICOM data, cal: caliper, 3Dcal: 3D-scan and virtual linear measurements, pat: linear measurements on patient DICOM data; time of dissection (for cadaver studies): dissection is done before image acquisition (dis) or after image acquisition (nodis); could not be assigned to any of the introduced categories (other). A detailed description for each subcategory can be found in Appendix A

Descriptive analysis

The 3D-printing technology used is reported for all publications that evaluate *printing errors*. The proprietary technologies of manufacturers are categorized into the three main groups of the basic 3D-printing technologies: "curing of liquid photopolymers", "extrusion of tough masses through nozzle" and "melting/sintering/binding of powder" (Table 3).

Table 3 Basic 3D-printing technologies, printing technologies as named by manufacturer of device and description for each of them

Basic technology	Printing technology as described in publication or by manufacturer	Description
curing of liquid photopolymers	Multi jet printing (MJP) / Polyjet printing(PJP)	A photocurable polymer is released by a printhead and is directly cured afterwards by UV light.
	Digital light processing (DLP)	A build plate inside a tank filled with liquid resin is exposed with UV light from underneath. Each exposure adds a whole layer to the built plate. The buid plate moves upwards after every light exposure.
	Stereolithography (SLA)/Scan, Spin and Selectively Photocuring	Mirrors redirect a laser beam through a tank filled with a photocurable liquid resin.
	Lubricant sublayer photo curing	A build plate inside a tank filled with liquid resin is exposed with UV light from underneath. Each exposure adds a whole layer to the build plate. The buid plate moves upwards after every light exposure. A lubricant is added to prevent the printed part from sticking to the membrane between the part and projector.
	Liquid-crystal display printing (LCD)	A build plate inside a tank filled with liquid resin is exposed with UV light from underneath. Areas which should not polymerize are covered from the curing light by a LCD screen.
	Continuous liquid interface production (CLIP)	A build plate inside a tank filled with liquid resin is exposed constantly with UV light from underneath and constantly moving upwards. An oxygen permeable membrane prevents the printed parts from sticking to the bottom of the tank.
extrusion of tough masses through nozzle	Fused deposition modeling (FDM) / fused filament fabrication (FFF)	A filament of a thermoplastic polymer is extruded through a hot nozzle.
melting/sintering/ binding of powder	Selective laser sintering (SLS)	A powder is spread layer by layer and sintered by a laser.
	Selective laser melting (SLM)	A metal powder is spread layer by layer and melted by a laser.
	Color jet printing (CJP)	Powder is spread layer by layer and (colored) binder is added through the printhead.

For all publications that evaluate printing errors, a subgroup analysis is performed for the basic printing technology used within every type of original structure

Quantitative analysis

In a further step the literature is screened for measurements of linear deviations in medical 3D-printing processes. If average values are stated by the authors, the *absolute values of maximum mean deviation* (*AMMD*) per publication are reported. According to Eq. 1, the metric *AMMD* is defined as the absolute value of the largest avarage linear deviation. In Eq. 1, $\bar{x}$ represents avarage values of liner deviations and $i=1$ to $i=n$ the the number of parameters analyzed per publication.

$$AMMD = \max_{i=1}^{n}(|\bar{x}_i|) \qquad (1)$$

All values are reported individually for the main types of error (SegE, SegC, DEE, PrE, IAE) and their combinations, respectively. For the most frequently evaluated *partial error* (*printing error*, PrE) and the most frequently evaluated *combined error* (*total error*, SegE+DEE + PrE), a more detailed analysis is performed: AMMD are reported individually for each of their described sub-categories.

Results

Descriptive analysis

Since 2015, with seven publications meeting the inclusion criteria in that year, the amount of relevant publications has increased significantly. A preliminary peak is to be found in 2021, when 28 publications investigating geometric accuracy of medical 3D-printing were published. By December 4th 2022, a total of 139 investigations are identified. They are often specific to anatomical regions or artificial test specimen and are listed here according to descending prevalence: teeth or jaws without other bones of skull ($n=52$), skull bones without jaw ($n=17$), heart and coronary arteries ($n=16$), artificial test specimen ($n=13$). The following with less than $n=9$ per region: bones of upper limb, brain vessels, bones of lower limb, pelvic bones, liver with bile ducts and / or gall bladder, thoracic aorta, kidney, animals, vertebrae or spine column, abdominal vessels, brain parenchyma, prostate, trachea or bronchial system, uterus, outer ear and nasal airways. By far the

largest number of investigations are carried out in the field of dentistry (approximately one third of all included publications investigate structures that belong to the group "teeth or jaw without other skull bones").

Publications evaluating printing errors are analyzed for the printing technologies used. Figure 6 shows the number of publications per proprietary printing technology for all of them as named by manufacturers. Figure 12 in Appendix B additionally shows the proportion of basic printing technologies per type of original structure.

Each publication is analyzed for the type of error evaluated, the measurement methods and the experimental setup of the image acquisition. Based on this analysis all publications are assigned to at least one of the defined categories. In the following section, the subcategories for the detailed analysis of the applied methods, together with the publications assigned to them, are shown for each main type of error and their possible combinations in Table 4 to Publications that evaluate the DEE and the PrE in combination are organized by applied methods and shown in Table 9. The same categories as described for the individual evaluation of the PrE are adopted. The only difference is that the direct result of segmentation is used as a reference instead of the print-STL.

Table 9. Publications that evaluate the total error (SegE+DEE+PrE) are shown separately in Table 10.

Publications that evaluate the SegE individually are organized by applied methods and shown in Table 4.

Publications that evaluate the DEE individually are organized by applied methods and shown in Table 5.

Publications that evaluate the PrE individually are organized by applied methods and shown in Table 6.

Publications that evaluate the IAE and SegC individually are shown in Table 7.

Publications that evaluate the SegE and the DEE in combination are organized by applied methods and shown in Table 8. The same categories as described for the individual evaluation of the SegE are adopted. The only difference is that the print-STL is compared with the original structure instead of the direct segmentation result.

Publications that evaluate the DEE and the PrE in combination are organized by applied methods and shown in Table 9. The same categories as described for the individual evaluation of the PrE are adopted. The only difference is that the direct result of segmentation is used as a reference instead of the print-STL.

According to our categorization, SegE experiments are categorized based on two key factors: 1. the measurement method employed, such as surface deviation analysis or linear measurements and 2. the imaging setup, which involves, among other aspects, distinguishing between phantom or cadaver studies.

In contrast, when subdividing experiments to assess the PrE, only the measurement methods used are considered, as the imaging setup does not influence this aspect. Conversely, subdividing experiments that evaluate the *total error* is more intricate due to the involvement of
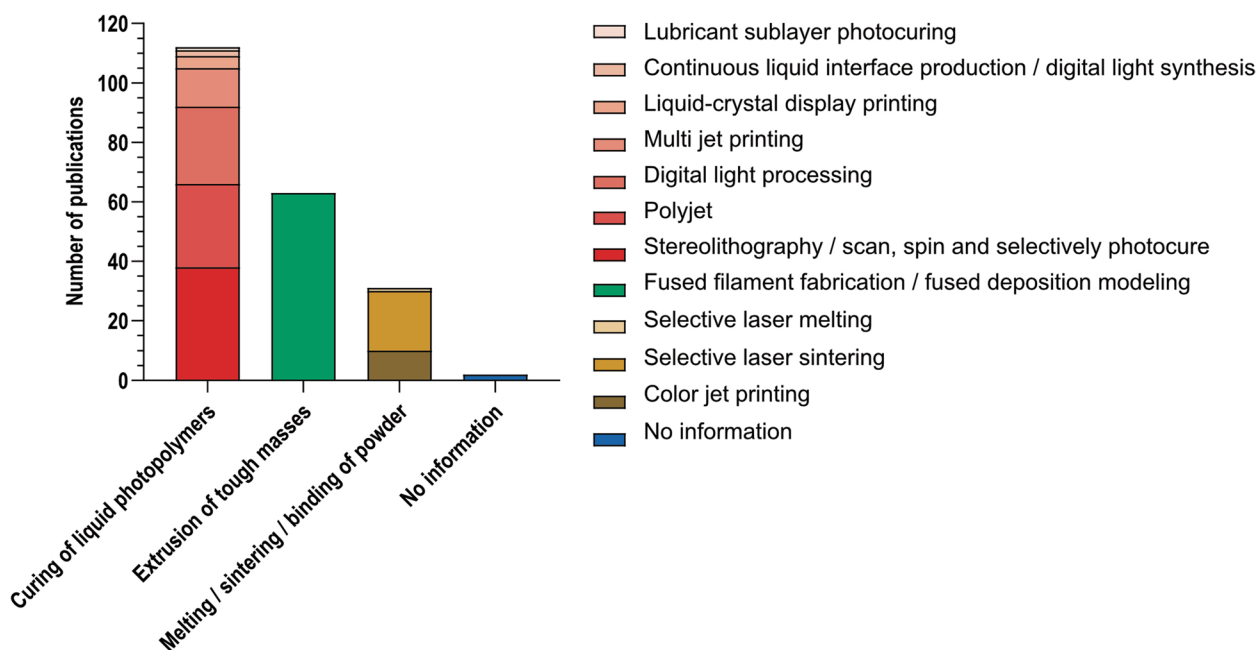

Fig. 6 Printing technologies used within publications that assess the printing error. Absolute number of publications by printing technology as named by manufacturer of 3D-printer. Note that codominance of two or more printing technologies within one publication is possible

Table 4 SegE evaluation. Publications according to the subcategories for the detailed analysis of applied methods as introduced in chapter 2.2.10. and visualized in Fig. 5. n.a. = not applicable, for subcategories no publication could be assigned to

Basic Approach	Imaging Setup	Tools for Linear Measurements	Time of Dissection	Publications
lin	**nosim**	cal		n.a.
		3Dcal		n.a.
	sim	cal		n.a.
		3Dcal		n.a.
	cad	cal	dis	[69]
			nodis	[15, 70, 71]
		3Dcal	dis	n.a.
			nodis	n.a.
	pat			n.a.
surf	nosim			n.a.
	sim			n.a.
	cad		dis	[72, 73]
			nodis	[74, 75]
other				[29, 74–77]

basic approach: linear (lin) or surface (surf) deviation based analysis; imaging setup: experimental setups of the image acqusition: nosim: artifical model and no simulation of adjacent tissue, sim: artifical model and simulation of adjacent tissue, cad: cadaver study, pat: scan of patients due to clinical questions; tools for linear measurements: cal: caliper, 3Dcal: 3D-scan and virtual linear measurements, pat: linear measurements on patient DICOM data; time of dissection (for cadaver studies): dissection is done before image acquisition (dis) or after image acquisition (nodis); could not be assigned to any of the introduced categories (other)

Table 5 DEE evaluation. Publications according to the subcategories for the detailed analysis of applied methods as introduced in chapter 2.2.10. and visualized in Fig. 5

Basic Approach	Publications
lin	[70]
surf	[78]
other	[79]

basic approach: linear (lin) or surface (surf) deviation based analysis; could not be assigned to any of the introduced categories (other)

Table 6 PrE evaluation. Publications according to the subcategories for the detailed analysis of applied methods as introduced in chapter 2.2.10. and visualized in Fig. 5

Basic Approach	Tools for Linear Measurements	Publications
lin	**DICOM**	[80, 81]
	cal	[21, 69, 71, 82–101]
	3Dcal	[17, 31, 102–110]
surf		[17–19, 31, 85, 103, 105–128]
other		[129–141]

basic approach: linear (lin) or surface (surf) deviation based analysis; tools for linear measurements: DICOM: CT-Scan of 3D-printed model and linear measurements on resulting DICOM data, cal: caliper, 3Dcal: 3D-scan and virtual linear measurements; could not be assigned to any of the introduced categories (other)

three key factors: 1. The measurement tools employed to assess the original structure; 2. the imaging setup used and 3. the measurement tools employed to evaluate the printed model.

Table 7 IAE and SegC assessment

Main Types of Error	Publications
IAE	[15, 70, 71, 91, 100, 119, 126, 127, 142–146]
SegC	[126, 147–150]

Given that the SegE sub-categories encompass the first two key factors and the PrE subcategories encompass the third one, they can be integrated to form total error subcategories that encompass all three key factors. The complexity arising from the various combinations of SegE and PrE subcategories found in the literature is illustrated in (Fig. 7).

Table 10 shows all combinations of SegE subcategories (describing methods for measuring the original structures and setups of image acquisition) with PrE subcategories (those describe methods for measuring the printed model) found in the literature (Fig. 7). For each combination, the corresponding publications are listed.

Quantitative analysis

The *absolute values of maximum mean deviations* per publication (AMMD) are illustrated for each main type of error in Fig. 8. No mean values are found for the digital editing error. Mean values are not computed - only the values explicitly reported by the authors are presented. All five outliers are not displayed in Fig. 8: one printing error outlier (PrE) with a value of 6.44 mm [141] and four total

Table 8 combined evaluation of SegE and DEE. Publications according to the subcategories for the detailed analysis of applied methods as introduced in chapter 2.2.10. and visualized in Fig. 5. n.a. = not applicable, for subcategories no publication could be assigned to

Basic Approach	Imaging Setup	Tools for Linear Measurements	Time of Dissection	Publications
lin	**nosim**	cal		[151, 152]
		3Dcal		n.a.
	sim	cal		n.a.
		3Dcal		n.a.
	cad	cal	dis	[153]
			nodis	n.a.
		3Dcal	dis	n.a.
			nodis	n.a.
	pat	pat		[80, 81, 91, 95, 129, 134, 154, 155]
surf	nosim			n.a.
	sim			n.a.
	cad		dis	[156]
			nodis	n.a.
other				n.a.

basic approach: linear (lin) or surface (surf) deviation based analysis; imaging setup: experimental setups of the image acqusition: nosim: artifical model and no simulation of adjacent tissue, sim: artifical model and simulation of adjacent tissue, cad: cadaver study, pat: scan of patients due to clinical questions; tools for linear measurements: cal: caliper, 3Dcal: 3D-scan and virtual linear measurements, pat: linear measurements on patient DICOM data; time of dissection (for cadaver studies): dissection is done before image acquisition (dis) or after image acquisition (nodis); could not be assigned to any of the introduced categories (other)

Table 9 Combined evaluation of DEE and PrE. Publications according to the subcategories for the detailed analysis of applied methods as introduced in chapter 2.2.10. and visualized in Fig. 5. n.a. = not applicable, for subcategories no publication could be assigned to

Basic Approach	Tools for Linear Measurements	Publications
lin	**DICOM**	n.a.
	cal	n.a.
	3Dcal	n.a.
surf		n.a.
other		[157]

basic approach: linear (lin) or surface (surf) deviation based analysis; tools for linear measurements: DICOM: CT-Scan of 3D-printed model and linear measurements on resulting DICOM data, cal: caliper, 3Dcal: 3D-scan and virtual linear measurements; could not be assigned to any of the introduced categories (other)

error outliers (SegE+DEE + PrE) with values of 3.0 mm [165], 3.8 mm [183], 3.81 mm [95] and 4.8 mm [170].

The green box in Fig. 8 shows the AMMD for the printing error. A more detailed analysis of the printing error including the subcategories can be found in Fig. 9. All three outliers are not displayed in Fig. 9: One caliper group outlier (PrE_lin_cal) with a value of 1.16 mm [95], one 3D-scan and surface comparison group outlier (PrE_surf) with a value of 0.633 mm [113] and one outlier in the group of heterogenous approaches (PrE_other) with a value of 6.44 mm [141].

The yellow box of Fig. 8 shows the AMMD for the *total error* (SegE+DEE + PrE). A more detailed analysis of the total error including the combinations of SegE and PrE subcategories can be found in Fig. 10.

Discussion

In terms of quality assurance in medical 3D-printing the field of dentistry accounts for the largest proportion of all publications (37%). This is primarily due to the relatively long history of CAD/CAM (Computer-Aided Design/Computer-Aided Manufacturing) processes in dentistry. A historical perspective of CAD/CAM development in dentistry is provided by Miazaki et al., starting in 1971 with the utilization of computer-guided subtractive manufacturing machines for crown production based on optical impressions [202]. The CAD/CAM process then paved the way for the integration of additive manufacturing techniques in dentistry, earlier than in other medical fields. Rekow has also highlighted the role of additive manufacturing in "digital dentistry" [203].

In our findings liquid photopolymer curing is generally the most employed basic printing technology. In dentistry, the use of SLA (Stereolithography), DLP (Digital Light Processing), or PJP (PolyJet Printing) is prevalent. These methods offer advantages such as short production times, high surface resolution, and mechanical durability [204]. FFF (Fused Filament Fabrication) represents the largest category of individual technologies. Overall, FFF-based processes

Table 10 total error (SegE+DEE+PrE) evaluation. Publications according to the combinations of subcategories of the segmentation error (describing methods for measuring the original structures and setups of image acquisition) and the printing error (describing methods for measuring the printed model). All combinations found in the literature are listed. Combinations no publications could be assigned to are not shown

Segmentation Error				Printing Error		Publications
basic approach	imaging setup	tools for linear measurements	time of dissection	basic approach	tools for linear measurements	
lin	**nosim**	**cal**		lin	cal	[121, 134, 144, 152, 158–160]
	cad	cal	dis			[153, 161–166]
		cal	nodis			[15, 70, 71, 167]
		3Dcal	nodis		3Dcal	[168]
	pat				DICOM	[80, 81, 137, 141, 169–178]
	pat				cal	[95, 146, 154, 155, 179–190]
	pat			other		[129, 142, 171, 191–194]
surf	nosim			surf		[119, 195–198]
	cad		dis			[72]
			nodis			[125]
other				lin	DICOM	[199]
					cal	[93, 99, 100, 145, 200]
				surf		[201]
				other		[142]

basic approach: linear (lin) or surface (surf) deviation based analysis; imaging setup: experimental setups of the image acqusition: nosim: artifical model and no simulation of adjacent tissue, sim: artifical model and simulation of adjacent tissue, cad: cadaver study, pat: scan of patients due to clinical questions; tools for linear measurements: DICOM: CT-Scan of 3D-printed model and linear measurements on resulting DICOM data, cal: caliper, 3Dcal: 3D-scan and virtual linear measurements, pat: linear measurements on patient DICOM data; time of dissection (for cadaver studies): dissection is done before image acquisition (dis) or after image acquisition (nodis); could not be assigned to any of the introduced categories (other)

are the most cost-effective and easiest to use. They are well-suited for initial exploration of 3D-printing and at the same time enable the production of finalized products and sterilizable implants [205]. In contrast, the least studied techniques are powder-based. This is likely because they are cost-intensive and most complex to implement. Their application requires a substantial allocation of resources and specific technical expertise, which can be limited in clinical settings. Illi et al. provided a comprehensive overview of a cardiovascular phantom production process, including reporting on the 10 largest studies concerning geometric accuracy [14]. Among these, material jetting and stereolithography are the most widely used 3D-printing technologies, which is consistent with our findings.

Among the *partial errors*, DEE as *digital editing error* is the least studied, while PrE as *printing error* is the most studied. Nevertheless, our results allow for an initial assessment of DEE in terms of its impact on the *total error*. The SegE was even studied significantly less often than the PrE, although the SegE seems to be much more influenced by manual input. When assessing the segmentation process, a distinction is made between publications in which the direct segmentation result was compared to the original structure (SegE) and those in which the segmentation was further processed (SegE+DEE), for example, using digital editing techniques such as smoothing. Analyzing the

deviations in both groups, their values do not differ greatly. This may indicate that standard digital editing techniques such as smoothing or artefact removal could have a minor impact on the *total error* of the production process. This assumption is supported by results from Ionata et al. presenting the only available AMMD for the combination of *digital editing error* and *printing error* (DEE+PrE): with a value of 0.12 mm [157], it is close to the lower end of the range of values obtained for the isolated printing error (PrE). However, further research is needed to quantify the influence of DEE, as only three publications are found that individually address this error.

Segmentation Error (SegE) is often evaluated using linear measurements. However, in the literature it is often not clear whether the original structure was compared to the direct segmentation result or to the *print-STL*. For future investigations, it would be beneficial to strive for more concise reporting. Our categorization of SegE is based on two dimensions: the measurement methods used and the imaging setup, enabling an assessment of the applied methods in terms of accuracy and realism:

The least accurate measurement method is the comparison of linear measurements on multi-planar reconstructions of slice images with corresponding linear measurements of the segmentation result (SegE_lin_pat). The most accurate measurement method is surface
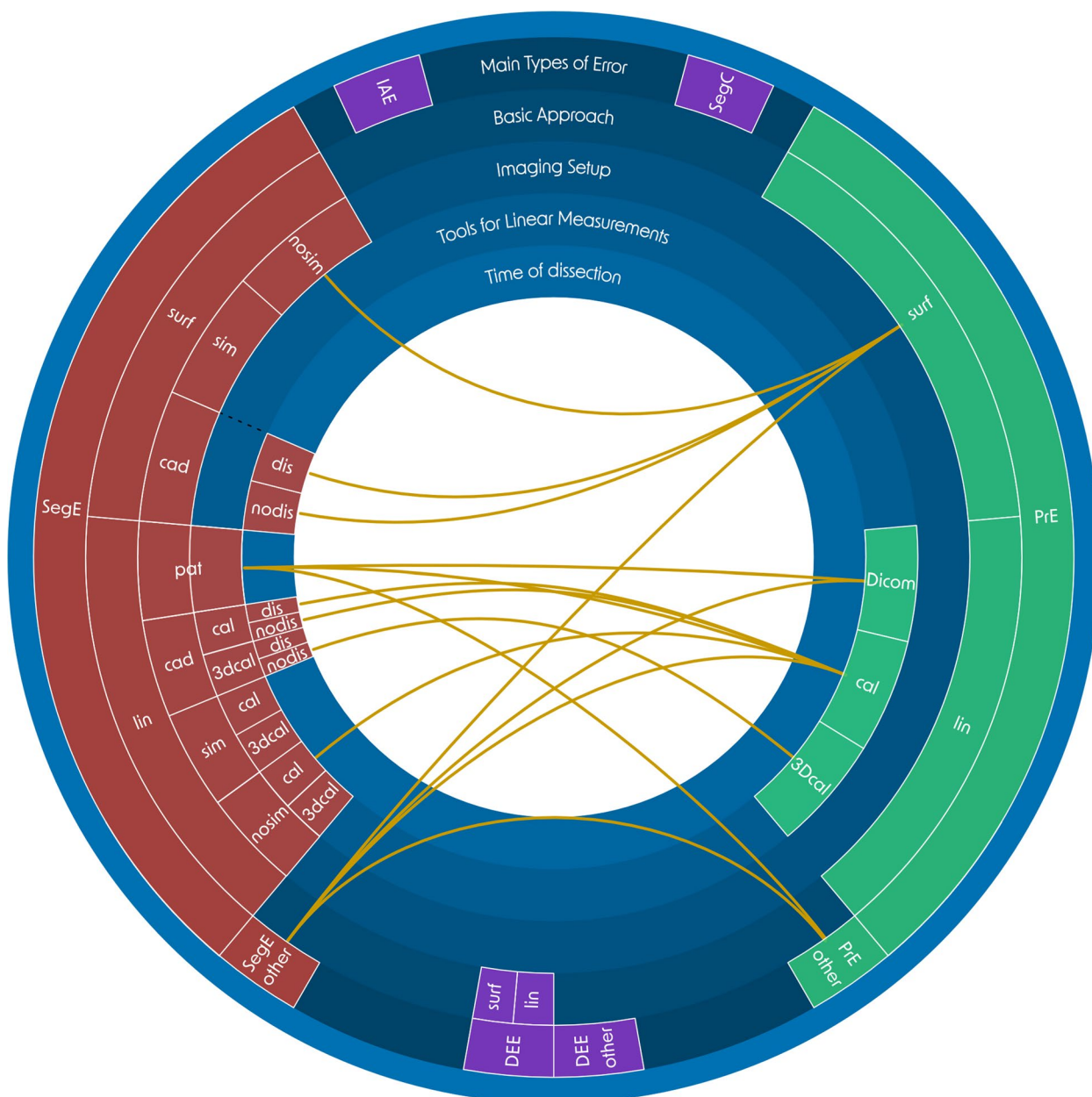
Fig. 7 Total error assessment. All combinations of SegE subcategories (describing methods for measuring the original structures and setups of the image acquisition) with PrE subcategories (describing methods for measuring the printed models), which are found in the included literature. Basic approach: linear (lin) or surface (surf) deviation based analysis; imaging setup: experimental setups of the image acqusition: nosim: artifical model and no simulation of adjacent tissue, sim: artifical model and simulation of adjacent tissue, cad: cadaver study, pat: scan of patients due to clinical questions; tools for linear measurements: DICOM: CT-Scan of 3D-printed model and linear measurements on resulting DICOM data, cal: caliper, 3Dcal: 3D-scan and virtual linear measurements, pat: linear measurements on patient DICOM data; time of dissection (for cadaver studies): dissection is done before image acquisition (dis) or after image acquisition (nodis); could not be assigned to any of the introduced categories (other)

deviation analysis between a 3D-scan of the original structure and the segmentation result.

The least realistic imaging setup is scanning artificial models in air, while the most realistic one involves scanning real patients for a clinical assessment (Fig. 11).

George et al. noted that the deviation of the segmentation process may be significantly lower when the original structures are scanned in air compared to in situ image acquisition [67]. This can pose a challenge: The most realistic imaging setup can only be combined with the least
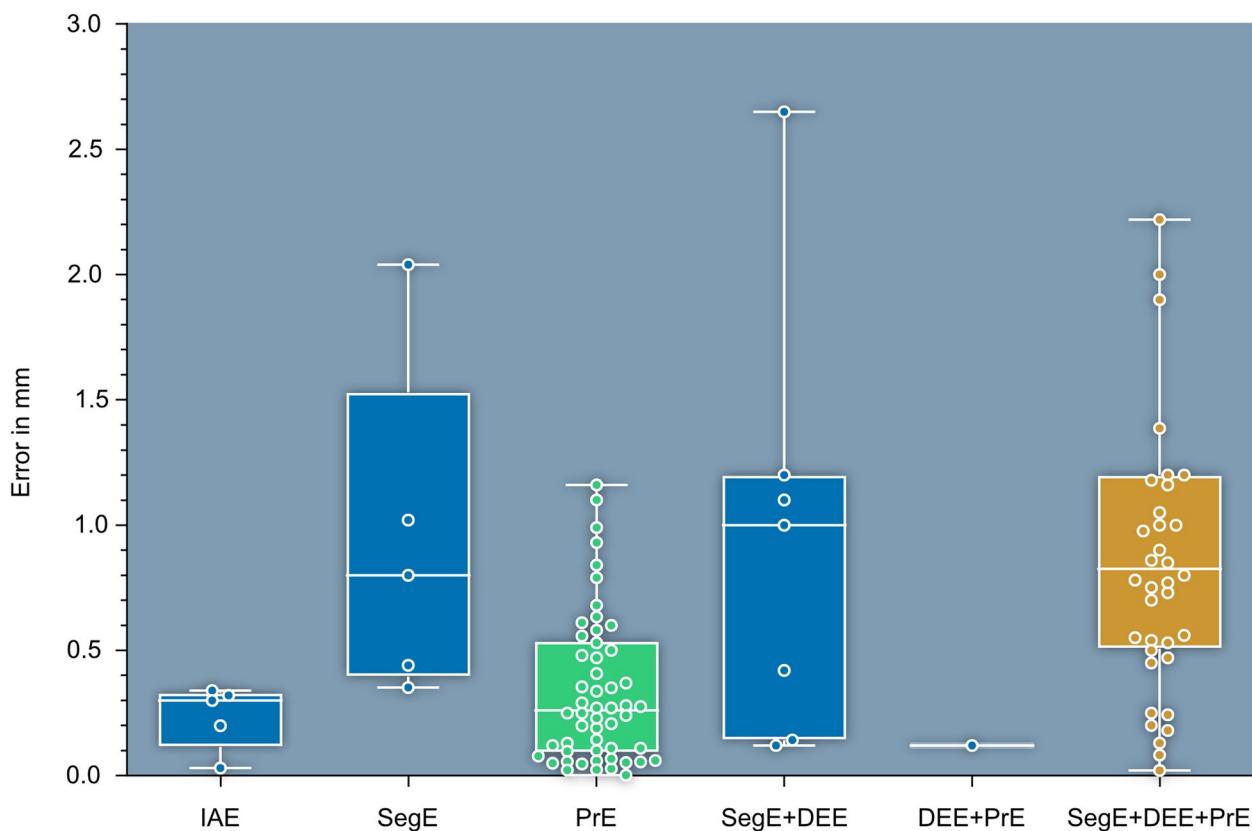
Fig. 8 AMMD, organized by main types of error and their combinations. IAE: *Image Acquistion Error*, SegE: *Segmentation Error*, DEE: *Digital Editing Error*, PrE: *Printing Error*. PrE (green) is the most frequently evaluated *partial error* and SegE+DEE + PrE (yellow) is the most frequently evaluated *combined error*

accurate measurement method. Therefore, a viable compromise is desirable. Cadaver studies have frequently been employed for this purpose as gold-standard [15, 69, 74]. These involve the dissection of soft tissue before or after imaging to allow reference measurements on the target structure of the segmentation (*original structure*). However, cadaver studies are expensive, personnel-intensive and need ethical approval in advance.

An accurate and realistic assessment of SegE can generally be defined as follows: A complex three-dimensional (anatomical) structure is surrounded by randomly arranged isodense structures during imaging. It is then segmented, and a 3D-scan of the original structure is compared with the direct segmentation result via surface comparison. Based on this definition, cadaver studies may not be the optimal method to evaluate SegE, considering the enormous efforts. To overcome these obstacles, future endeavours could focus on developing simple segmentation models that use artificial (3D-printed anatomical) structures and simulate adjacent (soft-) tissue.

Regarding combined errors, the combination of DEE and PrE has been studied the least, while the *total error* has been studied the most. Since the *total error* includes

SegE, among others, similar challenges arise. Figure 7 illustrates methods for evaluating the *total error* that are found in the literature. They range from simple and inexpensive methods (e.g. scanning an artificial model in air combined with a comparison of linear measurements taken on the original structure and the printed model) to the current gold-standard (scanning of cadaveric specimen, combined with a surface comparison between a 3D-scan of the *original structure* after dissection and a 3D-scan of the *printed model*). Besides cost, personnel and ethical aspects a limited availability has to be considered, too.

As a consequence, the need for alternatives seems justified. The combination of an artificial original structure with simulated adjacent tissue could be a promising solution that can be expected to achieve comparable accuracy and realism to cadaver studies but with significantly reduced cost and effort. Some attempts have been described in the literature to simulate adjacent tissue to increase the realism of the segmentation process [77, 156]. However, those still involve the use of cadaveric specimens: Van Eijnatten et al. embedded a human dry skull in silicone to simulate soft tissue for validating the influence of the head position during cone-beam CT [156]. Zhang
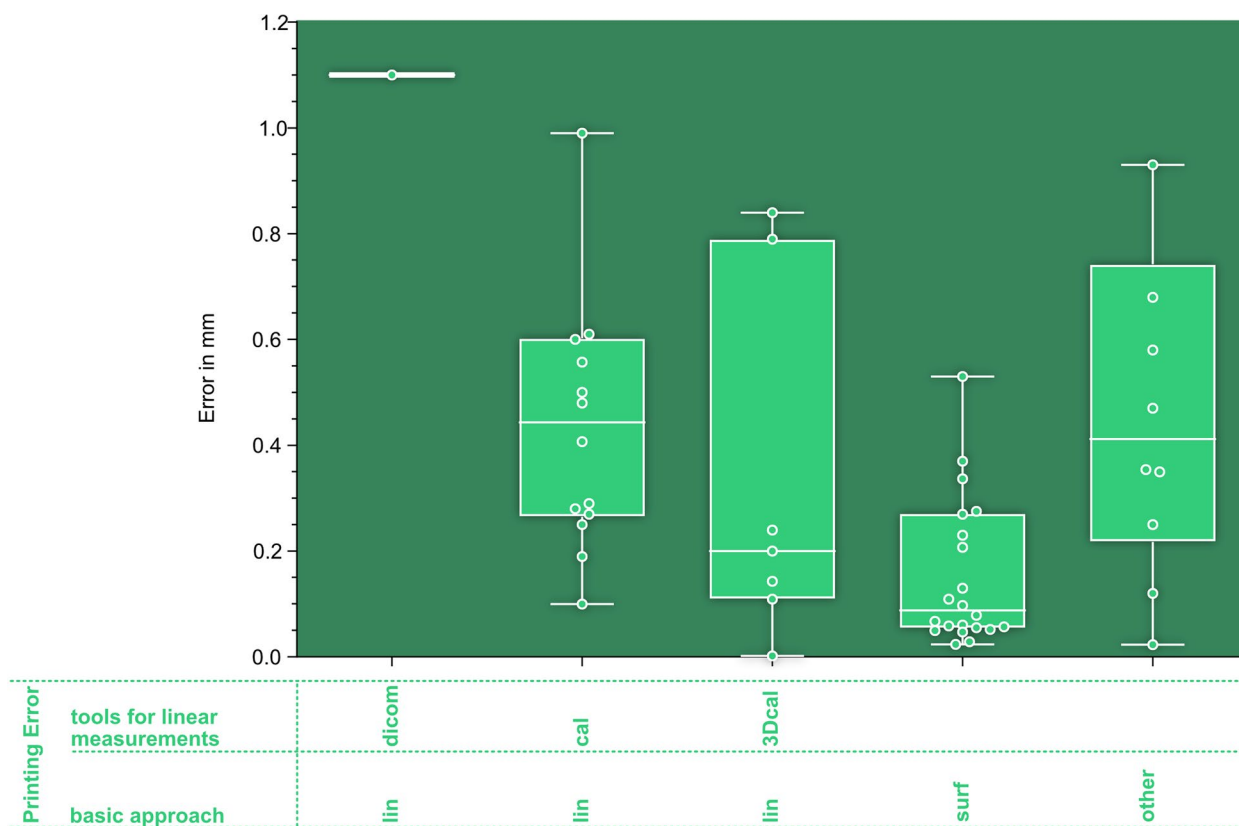
Fig. 9 Evalutation of printing errors. AMMD, organized by subcategories of the PrE. basic approach: linear (lin) or surface (surf) deviation based analysis; tools for linear measurements: DICOM: CT-Scan of 3D-printed model and linear measurements on resulting DICOM data, cal: caliper, 3Dcal: 3D-scan and virtual linear measurements; could not be assigned to any of the introduced categories (other)

et al. [77] placed artificial models of nasal airways inside a dry skull to use them as a realistic benchmark for the validation of their segmentation algorithm.

Judging by literature, the impression is that the preferred methods to investigate the *total error* are based on linear measurements on DICOM datasets of real patients. These methods offer the advantage that no experimental imaging is required. Instead, one can easily access the clinical database after obtaining ethical approval to use existing data. Nevertheless, methods involving patient data are associated with a serious weakness: reference measurements are limited to the least accurate method (linear measurements on multi planar reconstructions).

The data points in Fig. 8 are referenced to different publications. However, their deviation values for the *total error* are not significantly larger than for the *partial errors*. This may indicate that some of the partial errors compensate for each other. This is particularly relevant in a clinical environment where numerous specialist disciplines are often involved in the production of a 3D-printed patient-specific anatomical model, especially when considering that in some cases not all process steps may be the responsibility of the technician. For instance, technicians could have

two options for digital editing: 1. They receive the DICOM dataset and perform the segmentation themselves, or 2. they receive a completed segmentation from a clinician. Assuming the latter, a technician could document a very high result quality for the production process, e.g. because it relies on a significantly positive SegE and a significantly negative PrE. The expected high quality of results would no longer be guaranteed if the segmentation generates a strongly negative SegE. It can be concluded that assessing process quality solely based on the total error without knowledge of the partial errors is insufficient.

Although only one AMMD was found for the PrE_lin_ DICOM group in Fig. 8, it provides an indication of the hierarchy of measurement accuracies for PrE determination. The dispersion and the median values of the measurements decrease from left to right, corresponding to an increase in the accuracy of the measuring instrument. Linear measurements on DICOM datasets are the least accurate, surface deviation analyses are the most accurate. Nevertheless, it is important to consider that reporting the mean deviation of a surface deviation analysis alone tends to overestimate precision, as the value might be low even if the evaluated *process precision* itself is poor. This can happen when a
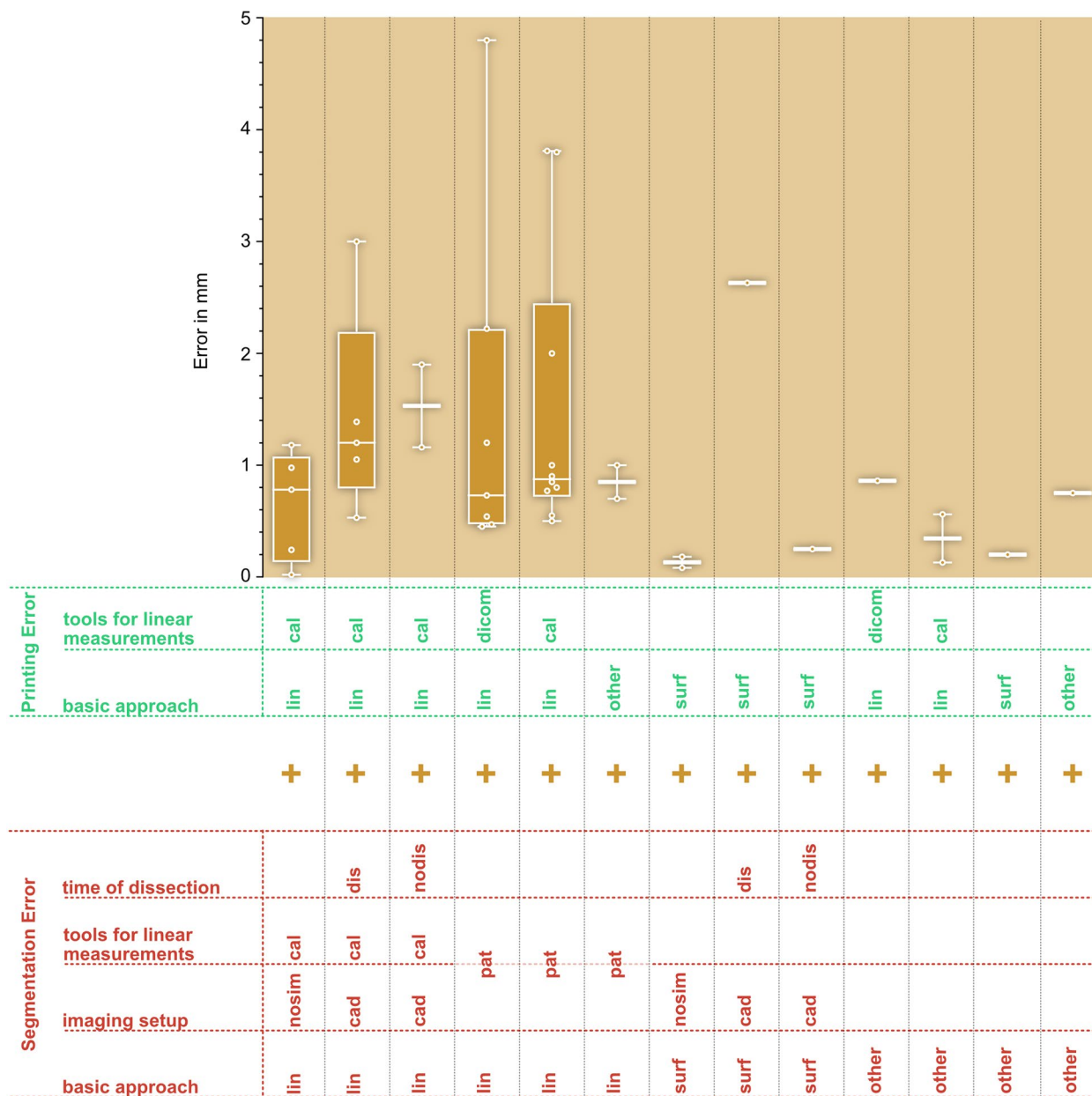
Fig. 10 Evalutation of total errors. AMMD, organized by combination of subcategories of the *segmentation error* (describing methods for measuring the original structures and setups of image acquisition) and the *printing error* (describing methods for measuring the printed model) as shown in Fig. 7 and Table 10 basic approach: linear (lin) or surface (surf) deviation based analysis; imaging setup: experimental setups of the image acqusition: nosim: artifical model and no simulation of adjacent tissue, sim: artifical model and simulation of adjacent tissue, cad: cadaver study, pat: scan of patients due to clinical questions; tools for linear measurements: DICOM: CT-Scan of 3D-printed model and linear measurements on resulting DICOM data, cal: caliper, 3Dcal: 3D-scan and virtual linear measurements, pat: linear measurements on patient DICOM data; time of dissection (for cadaver studies): dissection is done before image acquisition (dis) or after image acquisition (nodis); could not be assigned to any of the introduced categories (other)

high number of measurement points can lead to the summative elimination of positive and negative deviations. The discriminatory power of a surface deviation analysis can be significantly improved when the surface proportion within a tolerance based on clinical requirements is reported, as demonstrated by Lo Giudice et al. [148], Jin et al. [198] and Akyalcin et al. [103]. Specific tolerances for 3D-printing, tailored to anatomical regions and clinical demands, could be derived from minimal requirements for the registration in computer-assisted surgery ("navigation"), which range from 0.5 mm for spinal screw insertion to 2 mm in pelvic bone tumor resection [206–208].
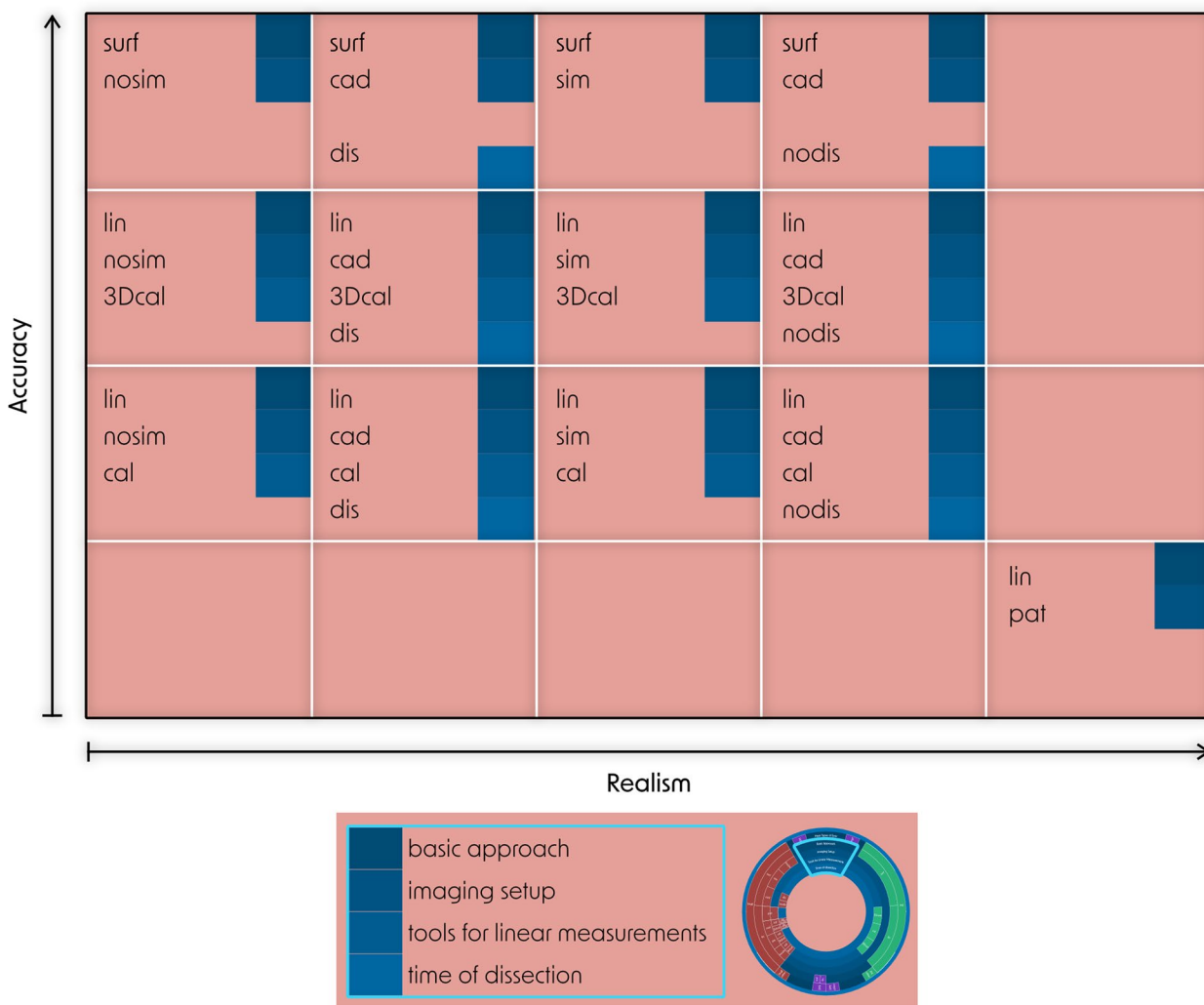
Fig. 11 Accuracy and realism of SegE subcategories, according to the subcategories for the detailed analysis of applied methods as introduced in chapter 2.2.10. and visualized in Fig. 5. Accuracy is mainly influenced by the basic approach and tools for linear measurements, while realism is mainly influenced by imaging setup and time of dissection. Basic approach: linear (lin) or surface (surf) deviation based analysis; imaging setup: experimental setups of the image acqusition: nosim: artifical model and no simulation of adjacent tissue, sim: artifical model and simulation of adjacent tissue, cad: cadaver study, pat: scan of patients due to clinical questions; tools for linear measurements: cal: caliper, 3Dcal: 3D-scan and virtual linear measurements, pat: linear measurements on patient DICOM data; time of dissection (for cadaver studies): dissection is done before image acquisition (dis) or after image acquisition (nodis)

That aspect is further illustrated in Fig. 10: Although only a small number of values is found for the group "SegE_surf_nosim - PrE_surf" their median value and dispersion are low. This group involves image acquisition of artificial models in air and a surface comparison between the 3D-scan of the *original structure* and the 3D-scan of the *printed model*. As a result, the least realistic imaging setup, with its associated minimal segmentation error, is combined with the measurement tool that tends to produce the lowest values.

Generally, the deviations are within the low single-digit millimeter range, which agrees with findings from Chae et al. They focused on 19 publications that evaluate the accuracy of medical 3D-printing using cadaveric specimens and linear measurements [15].

On the level of main types of errors five outliers are not displayed in Fig. 8. One PrE outlier (green box) is not displayed which is presented by Witowski et al., with a value of 6.44 mm [141]. Two reasons may explain this higher value compared to the rest of the literature: Firstly, their production process appears to be prone to potential inaccuracies (3D-printing of multi-part moulds, followed by assembly of the moulds and casting with silicone [209]). Secondly, they employ a measurement method of questionable accuracy: They acquire CT scans of the models, segment them and then, after alignment, perform a surface comparison

between the patient segmentation and the model segmentation. Figure 8 shows that the variance and the median values are larger for segmentation errors (SegE) than for printing errors (PrE). The error associated with the measurement principle (image acquisition followed by segmentation and surface comparison) appears to be larger than the expected error size here. A similar approach was chosen by other authors [130, 132, 134, 135, 137]. However, it is generally questionable whether slice image acquisition followed by segmentation is a valid tool to perform a surface deviation-based evaluation of the printing error. The same applies to the comparison of linear measurements between patient and model segmentation as described by Liang et al. [135].

Four total error outliers (Fig. 8, yellow box) are not displayed: those are presented by Silva et al. [165], Larguier et al. [183], Perica et al. [95] and Hedelin et al. [170] with values of 3.0 mm, 3.8 mm, 3.81 mm and 4.8 mm, respectively.

Several reasons might contribute to those comparatively high deviations: Some landmarks are difficult to identify for caliper measurements. In particular, if the model is scaled down for the 3D-print, this may result in a limited accuracy of the measurements. Larguier et al. for example validated their measurements in terms of accuracy and stated: "The caliper measurements of CD showed only moderate accuracy" [183]. Another aspect may be that the variety of dental publications leads to a relatively small average of measurements. As the focus is on absolute errors, which tend to be larger for bigger measurements, this could be an explanation for the relatively high value of some outliers. Future research may extend the present review to the analysis of relative errors.

Odeh et al. [210] defined checkpoints within the medical 3D-printing process at which measurements should be taken for quality assurance. They evaluated the *combined error* of segmentation and digital editing (SegE+DEE) as well as the *printing error* (PrE) and the *total error* (SegE+DEE+PrE). The same "checkpoints" are applied by Allan et al. and Perica et al. [80, 95]. Nevertheless, it should be noted that both only printed one model, which may limit the significance of their results.

In summary, there are various challenges in quality assurance for patient-specific 3D-printed anatomical models. These challenges can lead to either an overestimation or underestimation of the investigated errors. Particularly large or small values do not necessarily indicate exceptionally high or low accuracy; instead, the influence of the methods used for the evaluation should be critically examined. Future research should focus on developing realistic and resource-efficient segmentation models that also allow for high-accuracy measurements.

Recently published and upcoming standards address the early stage of maturity of nearly all additive manufacturing process categories, still resulting in strong deviations in some cases and a significant human-based error factor potential. The typical processual error reasons are missing process quality assurance, deviations in hardware, software, environmental conditions or feedstock. Therefore, the validation for accuracy should be part of the validation procedure. To assist this the first ISO/ASTM standards are published, e.g., ISO/ASTM 52901, 52,920, 52,930, 52,907, 529,004. Together with this review those will build a fundamental basis for a standardized qualification of the entire workflow.

Limitations

The literature search and the literature screening process was conducted by a single individual. The influence of the year of publication, the 3D-printing technology used as well as the image acquisition modalities or parameters on the geometric accuracy are not evaluated, which may be a relevant topic for future research. The publication focused solely on printing technologies and did not address specific printer models and their manufacturers. An interesting future research project could aim to investigate whether printers with 510(k) clearance are more accurate than printers without. The predominance of processes or printing technologies with a particularly high or low accuracy within some of our subcategories may cause bias for the deviation values.

Conclusions

This systematic review is an attempt to classify the literature regarding quality assurance of the geometric accuracy of patient-specific 3D-printed anatomical models into comparable categories. These are based on the measurement methods used and the experimental setups of the image acquisition.

In general, experimentally determined total errors do not appear to be significantly larger than partial errors. This suggests that partial errors may cancel each other out. Future research should therefore aim to investigate partial errors experimentally to describe the total error as the sum of the partial errors according to the rules of error propagation.

Current methods for quality assurance of the segmentation are either realistic and accurate or resource efficient. Future research should focus on implementing models that allow for evaluations with high accuracy and realism while being easy and cheap to perform. Those could also be used for further evaluation of influences of imaging parameters on the segmentation error.

Our system of categorization may be a valuable contribution to the structural design and reporting of future experiments as well as enhance the understanding of the overall process, not only for clinicians. It could support the training of specialists for risk assessment and process validation within the additive manufacturing industry.

Appendix 1

Evaluation of the Segmentation Error (SegE)

In the following methods are described which evaluate the SegE on basis of linear landmark measurements **(SegE_lin)**:

Medical images of an artificial structure (e.g. a 3D-printed anatomical model) are acquired without the simulation of the adjacent (soft) tissue. The structure is then segmented on the resulting DICOM images, and the original structure is compared with the segmentation result **(SegE_lin_nosim)**.

Linear measurements of landmarks are taken directly on the original structure with a caliper or a similar measuring tool and are compared with the corresponding digital measurements of the segmentation result **(SegE_lin_nosim_cal)**.

The original structure is 3D-scanned with an optical scanning system and digital linear measurements of landmarks are compared with the corresponding digital measurements of the segmentation result **(SegE_lin_nosim_3Dcal)**.

Medical images of an artificial structure (e.g. a 3D-printed anatomical model) are acquired with the simulation of the adjacent (soft) tissue. The structure is then segmented on the resulting DICOM images, and the original structure is compared with the segmentation result **(SegE_lin_sim)**.

Linear measurements of landmarks are taken directly on the original structure with a caliper or a similar measuring tool and are compared with the corresponding digital measurements of the segmentation result **(SegE_lin_sim_cal)**.

The original structure is 3D-scanned with an optical scanning system and digital linear measurements of landmarks are compared with the corresponding digital measurements of the segmentation result **(SegE_lin_sim_3Dcal)**.

Medical images of a cadaveric specimen are acquired. The cadaveric specimen is then segmented on the resulting DICOM images, and the original cadaver is compared with the segmentation result. To measure landmarks of the cadaver, it must be dissected. This can be done either prior to the image acquisition or after the image acquisition **(SegE_lin_cad)**.

The dissection is done prior to the image acquisition. Linear measurements of landmarks are taken directly on the cadaver with a caliper or a similar measuring tool and are compared with the corresponding digital measurements of the segmentation result **(SegE_lin_cad_cal_dis)**.

The dissection is done after the image acquisition. Linear measurements of landmarks are taken directly on the cadaver with a caliper or a similar measuring tool and are compared with the corresponding digital measurements of the segmentation result **(SegE_lin_cad_cal_nodis)**.

The dissection is done prior to the image acquisition. The structures of interest of the cadaver are 3D-scanned with an optical scanning system and digital linear measurements of landmarks are compared with the corresponding digital measurements of the segmentation result **(SegE_lin_cad_3Dcal _dis)**.

The dissection is done after the image acquisition. The structures of interest of the cadaver are 3D-scanned with an optical scanning system and digital linear measurements of landmarks are compared with the corresponding digital measurements of the segmentation result **(SegE_lin_cad_3Dcal _nodis)**.

Segmentation is conducted on original patient DICOM data and landmarks are measured on those. Linear measurements on DICOM data are compared with the corresponding digital measurements of the segmentation result **(SegE_lin_pat)**.

In the following methods are described which evaluate the SegE on basis of a surface deviation analysis. **(SegE_surf)**:

Medical images of an artificial structure (e.g. a 3D-printed anatomical model) are acquired without the simulation of the adjacent (soft) tissue. The structure is then segmented on the resulting DICOM images and the original structure is compared with the segmentation result. The original structure is 3D-scanned with an optical scanning system and the resulting digital model of the original structure is then compared with the segmentation result through surface deviation analysis after alignment **(SegE_surf_nosim)**.

Medical images of an artificial structure (e.g. a 3D-printed anatomical model) are acquired with the simulation of the adjacent (soft) tissue. The structure is then segmented on the resulting DICOM images and the original structure is compared with the segmentation result. The original structure is 3D-scanned with an optical scanning system and the resulting digital model of the original structure is then compared with the segmentation result through surface deviation analysis after alignment **(SegE_surf_sim)**.

Medical images of a cadaveric specimen are acquired. The cadaveric specimen is then segmented on the resulting DICOM images and the original cadaver is compared with the segmentation result. To perform a 3D scan of the cadavers' structures of interest, it needs to be dissected. This can be done either prior to the image acquisition or after the image acquisition **(SegE_surf_cad)**.

The dissection is done prior to the image acquisition. The structures of interest of the cadaver are 3D-scanned with an optical scanning system. The resulting digital model of the cadaver is then compared with the segmentation result through surface deviation analysis after alignment **(SegE_surf_cad_dis)**.

The dissection is done after the image acquisition. The structures of interest of the cadaver are 3D-scanned with an optical scanning system. The resulting digital model

of the cadaver is then compared with the segmentation result through surface deviation analysis after alignment (**SegE_surf_cad_nodis**).

Although this categorization approach covers the majority of experiments, some cannot be assigned to one of the categories. Those are summarized within the category **SegE_other**.

Evaluation of the Digital Editing Error (DEE)

Digital linear measurements of landmarks of the direct segmentation result are compared with corresponding digital linear measurements of the print-STL (**DEE_lin**).

Segmentation result and print-STL are compared through surface deviation analysis after alignment (**DEE_surf**).

Although this approach for categorization covers the majority of experiments some cannot be assigned to one of the categories. Those are summarized within the category **DEE_other**.

Evaluation of the Printing Error (PrE)

In the following methods are described which evaluate the PrE on basis of linear landmark measurements (**PrE_lin**):

CT scans of the printed model are acquired. Digital linear measurements of landmarks of the print-STL are compared with corresponding linear measurements on DICOM data of the printed model (**PrE_lin_DICOM**).

Digital linear measurements of landmarks of the print-STL are compared with corresponding direct measurements of the printed model, taken using a caliper or a similar measuring tool (**PrE_lin_cal**).

The printed model is 3D-scanned with an optical scanning system. Digital linear measurements of landmarks of the print-STL are compared with corresponding digital linear measurements of the printed model (**PrE_lin_3Dcal**).

In the following methods are described which evaluate the PrE on basis of a surface deviation analysis:

The printed model is 3D-scanned with an optical scanning system. The resulting digital model of the printed model is then compared with the print-STL through surface deviation analysis after alignment (**PrE_surf**).

Although this categorization approach covers the majority of experiments, some cannot be assigned to one of the categories. Those are summarized within the category **PrE_other**.

Evaluation of the Image Acquisition Error (IAE)

Medical images of an original structure are acquired. Linear measurements of landmarks are taken directly on the original structure with a caliper or a similar measuring tool and are compared with the corresponding linear measurements on DICOM data (**IAE**).

Segmentation Comparison Error (SegC)

Comparison of linear measurements of landmarks of different segmentation results with each other or comparison with each other through surface deviation analysis after alignment (**SegC**).

Combination of Segmentation Error and Digital Editing Error (SegE+DEE)

The combined error of segmentation and digital editing can be determined by measuring the original structure and comparing it to the print-STL. To achieve a more detailed classification the same categories as described for the individual evaluation of the segmentation error are adopted. The only difference is that the print-STL is compared with the original structure instead of the direct segmentation result.

If the authors did not specify whether they compared the original structure with the direct segmentation result or with the print-STL, it is assumed that they evaluated the segmentation error individually.

Combination of Digital Editing Error and Printing Error (DEE + PrE)

The combined error of digital editing and printing can be determined by measuring the direct segmentation result and comparing it to the printed model. To achieve a more detailed classification the same categories as described for the individual evaluation of the printing error are adopted. The only difference is that the direct result of segmentation is used as a reference instead of the print-STL.

Combination of Segmentation Error, Digital Editing Error and Printing Error (SegE+DEE + PrE)

The combined error of segmentation, digital editing and printing can be determined by measuring the original structure and comparing it with the printed model. These methods determine the overall error of the entire process. To achieve a more detailed classification, it is necessary consider methods for measuring both the original structure and the printed model. Additionally, it is important to consider the experimental setup of the image acquisition. Categories as described for the individual evaluation of the segmentation error describe methods to measure the original structure and the experimental setup of the image acquisition. Categories as described for the individual evaluation of the printing error describe methods to measure the printed model. Therefore, subcategories of segmentation errors and printing errors can be combined to provide a more detailed classification of measurements of the total error.
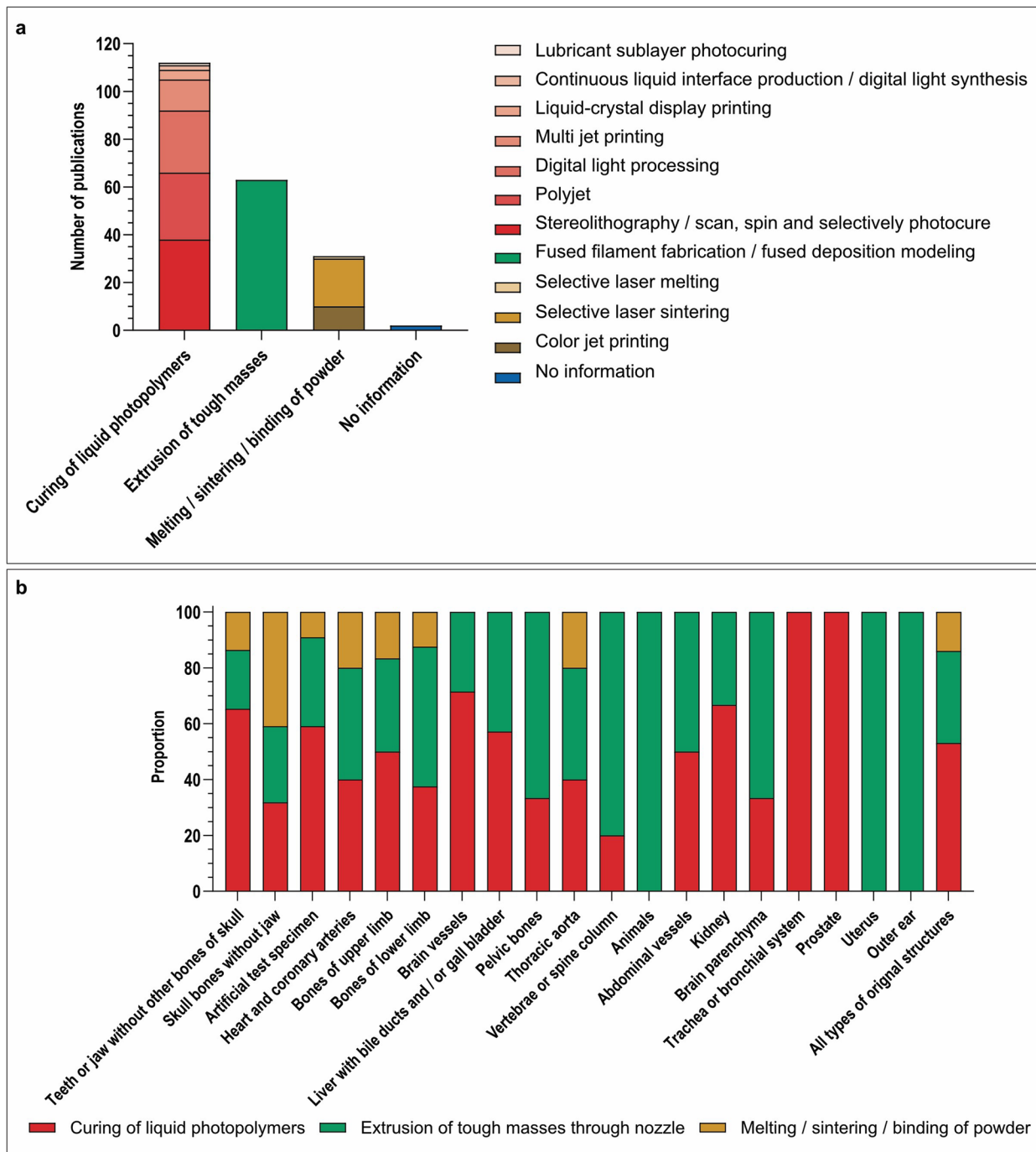
Appendix 2

Fig. 12 Used printing technologies within publications that assess the printing error. **a** absolute number of publications by printing technology as named by manufacturer of 3D-printer. **B** proportion of basic 3D-printing technologies by types of original structures. Right column: overall proportion of basic 3D-printing technologies. The groups "curing of liquid photopolymers", extrusion of tough masses through nozzle" and "melting/ sintering/binding of powder"are formed according to the main printing technologies as described in Table 3. Note that codominance of two or more printing technologies within one publication is possible

Abbreviations

SegE	Segmentation error
DEE	Digital editing error
PrE	Printing error
AMMD	Absolute values of the maximum mean deviation per publication
IAE	Image acquisition error
SegC	Segmentation comparison error
lin	Linear
surf	Surface
nosim	No simulation
sim	Simulation
cad	Cadaver
pat	Patient
cal	Caliper
3Dcal	3D-scan and virtual caliper
dis	Dissection
nodis	No dissection
DICOM	Digital imaging and communications in medicine
STL	Standard tessellation language
ISO	International organization for standardization
PRISMA	Preferred reporting items for systematic reviews and meta-analyses
RSNA	Radiological society of north america
MJP	Multi jet printing
PJP	Poly jet printing
DLP	Digital light processing
SLA	Stereolithography
LCD	Liquid crystal display
CLIP	Continuous liquid interface production
FDM	Fused deposition modeling
FFF	Fused filament fabrication
SLS	Selective laser sintering
SLM	Selective laser melting
CJP	Color jet printing
CAD	Computer aided design
CAM	Computer aided manufacturing

Supplementary Information

The online version contains supplementary material available at https://doi.org/10.1186/s41205-024-00210-5.

> **Additional file 1:.** High resolution version of the graphical abstract.

Availability of data and materials
No datasets were generated or analysed during the current study.

Declarations

Ethics approval and consent to participate
Not applicable.

Consent for publication
Not applicable.

Competing interests
The authors declare no competing interests.

Author details
[1]Department of General Orthopedics and Tumor Orthopedics, University Hospital Muenster, 48149 Münster, Germany. [2]Clinic for Radiology, University Hospital Muenster, 48149 Muenster, Germany. [3]Qualified AM GmbH, 82407 Wielenbach, Germany. [4]Department of Mechanical Engineering, Materials Engineering Laboratory, University of Applied Sciences Muenster, 48565 Steinfurt, Germany.

References

1. Schulze M, Gosheger G, Bockholt S, de Vaal M, Budny T, Tönnemann M, et al. Complex Bone tumors of the trunk-The role of 3D printing and navigation in tumor orthopedics: a case series and review of the literature. J Pers Med. 2021;11 https://doi.org/10.3390/jpm11060517.
2. Valls-Esteve A, Tejo-Otero A, Lustig-Gainza P, Buj-Corral I, Fenollosa-Artés F, Rubio-Palau J, et al. Patient-specific 3D printed soft models for liver surgical planning and hands-on training. Gels. 2023;9 https://doi.org/10.3390/gels9040339.
3. Wong A, Goonewardene MS, Allan BP, Mian AS, Rea A. Accuracy of maxillary repositioning surgery using CAD/CAM customized surgical guides and fixation plates. Int J Oral Maxillofac Surg. 2021;50:494–500. https://doi.org/10.1016/j.ijom.2020.08.009.
4. Yang C, Zhang C, Wu J, Xu X, Zhang Y, Zhang S. Three-dimensional printed customized surgical guides for the precise correction of complex Midfacial post-traumatic deformities. J Craniofac Surg. 2022;33:1150–3. https://doi.org/10.1097/SCS.0000000000008329.
5. Omar M, Schulze M, Bruns N, Kotrych D, Gosheger G, Ettinger M. Update 3D-Druck in der Chirurgie muskuloskeletaler Tumoren. Unfallchirurg. 2022;125:361–70. https://doi.org/10.1007/s00113-022-01160-5.
6. Kotrych D, Angelini A, Bohatyrewicz A, Ruggieri P. 3D printing for patient-specific implants in musculoskeletal oncology. EFORT Open Rev. 2023;8:331–9. https://doi.org/10.1530/EOR-23-0066.
7. Molinari G, Emiliani N, Cercenelli L, Bortolani B, Gironi C, Fernandez IJ, Presutti L, Marcelli E. Assessment of a novel patient-specific 3D printed multi-material simulator for endoscopic sinus surgery. Front Bioeng Biotechnol. 2022;10:974021. https://doi.org/10.3389/fbioe.2022.974021.
8. Chedid VG, Kamath AA, Knudsen JM, Frimannsdottir K, Yost KJ, Geske JR, Morris JM, Taner T, Matsumoto JM, Kamath PS. Three-dimensional-printed liver model helps learners identify hepatic subsegments: A randomized-controlled cross-over trial. Am J Gastroenterol. 2020;115:1906–10. https://doi.org/10.14309/ajg.0000000000000958.
9. Grab M, Hundertmark F, Thierfelder N, Fairchild M, Mela P, Hagl C, Grefen L. New perspectives in patient education for cardiac surgery using 3D-printing and virtual reality. Front Cardiovasc Med. 2023;10:1092007. https://doi.org/10.3389/fcvm.2023.1092007.
10. Joseph FJ, Vanluchene HER, Goldberg J, Bervini D. 3D-printed head model in Patient's education for Micro-neurosurgical aneurysm clipping procedures. World Neurosurg. 2023;175:e1069–74. https://doi.org/10.1016/j.wneu.2023.04.070.
11. Yammine K, Karbala J, Maalouf A, Daher J, Assi C. Clinical outcomes of the use of 3D printing models in fracture management: a meta-analysis

of randomized studies. Eur J Trauma Emerg Surg. 2022;48:3479–91. https://doi.org/10.1007/s00068-021-01758-1.

12. Meyer-Szary J, Luis MS, Mikulski S, Patel A, Schulz F, Tretiakow D, et al. The role of 3D printing in planning complex medical procedures and training of medical professionals-cross-sectional multispecialty review. Int J Environ Res Public Health. 2022;19 https://doi.org/10.3390/ijerph19063331.

13. Chepelev L, Wake N, Ryan J, Althobaity W, Gupta A, Arribas E, Santiago L, Ballard DH, Wang KC, Weadock W, et al. Radiological Society of North America (RSNA) 3D printing special interest group (SIG): guidelines for medical 3D printing and appropriateness for clinical scenarios. 3D Print Med. 2018;4:11. https://doi.org/10.1186/s41205-018-0030-y.

14. Illi J, Bernhard B, Nguyen C, Pilgrim T, Praz F, Gloeckler M, Windecker S, Haeberlin A, Gräni C. Translating imaging into 3D printed cardiovascular phantoms: A systematic review of applications, technologies, and validation. JACC Basic Transl Sci. 2022;7:1050–62. https://doi.org/10.1016/j.jacbts.2022.01.002.

15. Chae MP, Chung RD, Smith JA, Hunter-Smith DJ, Rozen WM. The accuracy of clinical 3D printing in reconstructive surgery: literature review and in vivo validation study. Gland Surg. 2021;10(2293–2303) https://doi.org/10.21037/gs-21-264.

16. International Organization for Standardization. Accuracy (trueness and precision) of measurement methods and results — Part 2: Basic method for the determination of repeatability and reproducibility of a standard measurement method; International Organization for Standardization, 2019 (ISO 5725-2:2019). Available online: https://www.iso.org/obp/ui/en/#iso:std:iso:5725:-2:ed-2:v1:en. Accessed 7 Sept 2023.

17. Kim S-Y, Shin Y-S, Jung H-D, Hwang C-J, Baik H-S, Cha J-Y. Precision and trueness of dental models manufactured with different 3-dimensional printing techniques. Am J Orthod Dentofacial Orthop. 2018;153:144–53. https://doi.org/10.1016/j.ajodo.2017.05.025.

18. Tsolakis IA, Papaioannou W, Papadopoulou E, Dalampira M, Tsolakis AI. Comparison in terms of accuracy between DLP and LCD printing Technology for Dental Model Printing. Dent J (Basel). 2022;10 https://doi.org/10.3390/dj10100181.

19. Eltes PE, Kiss L, Bartos M, Gyorgy ZM, Csakany T, Bereczki F, Lesko V, Puhl M, Varga PP, Lazary A. Geometrical accuracy evaluation of an affordable 3D printing technology for spine physical models. J Clin Neurosci. 2020;72:438–46. https://doi.org/10.1016/j.jocn.2019.12.027.

20. Bramlet M, Olivieri L, Farooqi K, Ripley B, Coakley M. Impact of three-dimensional printing on the study and treatment of congenital heart disease. Circ Res. 2017;120:904–7. https://doi.org/10.1161/CIRCRESAHA.116.310546.

21. Braian M, Jimbo R, Wennerberg A. Production tolerance of additive manufactured polymeric objects for clinical applications. Dent Mater. 2016;32:853–61. https://doi.org/10.1016/j.dental.2016.03.020.

22. Das P, Chetry B, Paul S, Bhattacharya SS, Nath P. Detection and quantification of phosphate in water and soil using a smartphone. Microchem J. 2022;172 https://doi.org/10.1016/j.microc.2021.106949.

23. Engelhardt S, Sauerzapf S, Preim B, Karck M, Wolf I, de Simone R. Flexible and comprehensive patient-specific mitral valve silicone models with chordae tendineae made from 3D-printable molds. Int J Comput Assist Radiol Surg. 2019;14:1177–86. https://doi.org/10.1007/s11548-019-01971-9.

24. Brodie CH, Spotts I, Reguigui H, Leclerc CA, Mitchell ME, Holzman JF, Collier CM. Comprehensive study of 3D printing materials over the terahertz regime: absorption coefficient and refractive index characterizations. Opt Mater Express. 2022;12:3379–402. https://doi.org/10.1364/OME.465820.

25. Equbal A, Sood AK, Ansari AR, Equbal MA. Optimization of process parameters of FDM part for minimiizing its dimensional inaccuracy. Int J Mech Prod Eng Res Dev. 2017;7:57–66.

26. de Boutray M, Cavalcanti Santos J, Bourgeade A, Ohayon M, Chammas P-E, Garrel R, Poignet P, Zemiti N. Fibular registration using surface matching in navigation-guided osteotomies: a proof of concept study on 3D-printed models. Int J Comput Assist Radiol Surg. 2022;17:1321–31. https://doi.org/10.1007/s11548-022-02608-0.

27. Fang C, Cai H, Kuong E, Chui E, Siu YC, Ji T, Drstvenšek I. Surgical applications of three-dimensional printing in the pelvis and acetabulum: from models and tools to implants. Unfallchirurg. 2019;122:278–85. https://doi.org/10.1007/s00113-019-0626-8.

28. Kunkel MH, Gebhardt A, Mpofu K, Kallweit S. Quality assurance in metal powder bed fusion via deep-learning-based image classification. Rapid Prototyp J. 2020;26:259–66. https://doi.org/10.1108/RPJ-03-2019-0066.

29. Chen MY, Woodruff MA, Dasgupta P, Rukin NJ. Variability in accuracy of prostate cancer segmentation among radiologists, urologists, and scientists. Cancer Med. 2020;9:7172–82. https://doi.org/10.1002/cam4.3386.

30. Lee AY, Patel NA, Kurtz K, Edelman M, Koral K, Kamdar D, Goldstein T. The use of 3D printing in shared decision making for a juvenile aggressive ossifying fibroma in a pediatric patient. Am J Otolaryngol - Head Neck Med Surg. 2019;40:779–82. https://doi.org/10.1016/j.amjoto.2019.07.001.

31. Gottsauner M, Reichert T, Koerdt S, Wieser S, Klingelhoeffer C, Kirschneck C, Hoffmann J, Ettl T, Ristow O. Comparison of additive manufactured models of the mandible in accuracy and quality using six different 3D printing systems. J Craniomaxillofac Surg. 2021;49:855–66. https://doi.org/10.1016/j.jcms.2021.04.003.

32. Cappellini C, Borgianni Y, Maccioni L, Nezzi C. The effect of process parameters on geometric deviations in 3D printing with fused deposition modelling. Int J Adv Manuf Technol. 2022;122:1763–803. https://doi.org/10.1007/s00170-022-09924-4.

33. Li Y, Min SW, Xie F, Zhang MY. A meta-analysis of clinical efficacy of preoperative use of three-dimensional printing in the treatment of tibial plateau fractures. Chin J Tissue Eng Res. 2021;25:1959–68. https://doi.org/10.3969/j.issn.2095-4344.3795.

34. Esplen N, Therriault-Proulx F, Beaulieu L, Bazalova-Carter M. Preclinical dose verification using a 3D printed mouse phantom for radiobiology experiments. Med Phys. 2019;46:5294–303. https://doi.org/10.1002/mp.13790.

35. Fanni BM, Sauvage E, Capelli C, Gasparotti E, Vignali E, Schievano S, Landini L, Positano V, Celi S. A numerical and 3D printing framework for the in vivo mechanical assessment of patient-specific cardiovascular structures. 2nd International Conference on Simulation for Additive Manufacturing, Sim-AM 2019; 2019. p. 31–9.

36. Gjelvold B, Mahmood DJH, Wennerberg A. Accuracy of surgical guides from 2 different desktop 3D printers for computed tomography-guided surgery. J Prosthet Dent. 2019;121:498–503. https://doi.org/10.1016/j.prosdent.2018.08.009.

37. Goetstouwers S, Kempink D, The B, Eygendaal D, van Oirschot B, van Bergen CJ. Three-dimensional printing in paediatric orthopaedic surgery. World J Orthop. 2022;13:1–10. https://doi.org/10.5312/wjo.v13.i1.1.

38. Hughes AJ, DeBuitleir C, Soden P, O'Donnchadha B, Tansey A, Abdulkarim A, McMahon C, Hurson CJ. 3D printing aids acetabular reconstruction in complex revision hip arthroplasty. Adv Orthop. 2017;2017:8925050. https://doi.org/10.1155/2017/8925050.

39. Imanian ME, Biglari FR. Modeling and prediction of surface roughness and dimensional accuracy in SLS 3D printing of PVA/CB composite using the central composite design. J Manuf Process. 2022;75:154–69. https://doi.org/10.1016/j.jmapro.2021.12.065.

40. Maragiannis D, Jackson MS, Igo SR, Chang SM, Zoghbi WA, Little SH. Functional 3D printed patient-specific modeling of severe aortic stenosis. J Am Coll Cardiol. 2014;64:1066–8. https://doi.org/10.1016/j.jacc.2014.05.058.

41. Minetola P, Eyers D. Energy and cost assessment of 3D printed Mobile case covers. Procedia CIRP; 2018. p. 130–5.

42. Singh D, Singh R, Boparai KS. Development and surface improvement of FDM pattern based investment casting of biomedical implants: A state of art review. J Manuf Process. 2018;31:80–95. https://doi.org/10.1016/j.jmapro.2017.10.026.

43. Sun Z, Wee C. 3D printed models in cardiovascular disease: an exciting future to deliver personalized medicine. Micromachines (Basel). 2022;13 https://doi.org/10.3390/mi13101575.

44. Xu J, Sheng H, Zhang S, Tan J, Deng J. Surface accuracy optimization of mechanical parts with multiple circular holes for additive manufacturing based on triangular fuzzy number. Front Mech Eng. 2021;16:133–50. https://doi.org/10.1007/s11465-020-0610-6.

45. Yi Z, He B, Liu Y, Huang S, Hong W. Development and evaluation of a craniocerebral model with tactile-realistic feature and intracranial pressure for neurosurgical training. J Neurointerv Surg. 2020;12:94–7. https://doi.org/10.1136/neurintsurg-2019-015008.

46. Yuan J, Tian J, Chen C, Chen G. Experimental investigation of color reproduction quality of color 3D printing based on colored layer features. Molecules. 2020;25 https://doi.org/10.3390/molecules25122909.

47. Langridge B, Momin S, Coumbe B, Woin E, Griffin M, Butler P. Systematic review of the use of 3-dimensional printing in surgical teaching and assessment. J Surg Educ. 2018;75:209–21. https://doi.org/10.1016/j.jsurg.2017.06.033.

48. Baumann F, Bugdayci H, Grunert J, Keller F, Roller D. Influence of slicing tools on quality of 3D printed parts. Comput-Aided Des Appl. 2016;13:14–31. https://doi.org/10.1080/16864360.2015.1059184.

49. Buda M, Bratos M, Sorensen JA. Accuracy of 3-dimensional computer-aided manufactured single-tooth implant definitive casts. J Prosthet Dent. 2018;120:913–8. https://doi.org/10.1016/j.prosdent.2018.02.011.

50. Chohan JS, Singh R, Boparai KS, Penna R, Fraternali F. Dimensional accuracy analysis of coupled fused deposition modeling and vapour smoothing operations for biomedical applications. Compos Part B. 2017;117:138–49. https://doi.org/10.1016/j.compositesb.2017.02.045.

51. Fastowicz J, Okarma K. Fast quality assessment of 3D printed surfaces based on structural similarity of image regions. 2018 International interdisciplinary PhD workshop, IIPhDW 2018; 2018. p. 401–6.

52. Hällgren S, Pejryd L, Ekengren J. 3D data export for additive manufacturing-improving geometric accuracy. Procedia CIRP; 2016. p. 518–23.

53. Hanson MS, Cozad BE, English JD, Kasper FK. Effects of accelerated aging on 3D-printed orthodontic model accuracy. J Clin Orthod. 2022;56:413–8.

54. Kenning KB, Risinger DC, English JD, Cozad BE, Harris LM, Ontiveros JC, Kasper FK. Evaluation of the dimensional accuracy of thermoformed appliances taken from 3D printed models with varied shell thicknesses: an in vitro study. Int Orthod. 2021;19:137–46. https://doi.org/10.1016/j.ortho.2021.01.005.

55. Aldosari S, Jansen S, Sun Z. Optimization of computed tomography pulmonary angiography protocols using 3D printed model with simulation of pulmonary embolism. Quant Imaging Med Surg. 2019;9(53–62) https://doi.org/10.21037/qims.2018.09.15.

56. Gopalan K, Tamir JI, Arias AC, Lustig M. Quantitative anatomy mimicking slice phantoms. Magn Reson Med. 2021;86:1159–66. https://doi.org/10.1002/mrm.28740.

57. Dlamini S, Chen Y-H, Jeffrey Kuo C-F. Complete fully automatic detection, segmentation and 3D reconstruction of tumor volume for non-small cell lung cancer using YOLOv4 and region-based active contour model. Expert Syst Appl. 2023;212 https://doi.org/10.1016/j.eswa.2022.118661.

58. Thereza-Bussolaro C, Lagravère M, Pacheco-Pereira C, Flores-Mir C. Development, validation and application of a 3D printed model depicting adenoid hypertrophy in comparison to a Nasoendoscopy. Head Face Med. 2020;16:5. https://doi.org/10.1186/s13005-020-00216-4.

59. de Armond CC, Lewis DD, Kim SE, Biedrzycki AH. Accuracy of virtual surgical planning and custom three-dimensionally printed osteotomy and reduction guides for acute uni- and biapical correction of antebrachial deformities in dogs. J Am Vet Med Assoc. 2022;260 https://doi.org/10.2460/javma.21.09.0419.

60. Choi E, Adams F, Palagi S, Gengenbacher A, Schlager D, Müller P-F, Gratzke C, Miernik A, Fischer P, Qiu T. A high-Fidelity phantom for the simulation and quantitative evaluation of transurethral resection of the prostate. Ann Biomed Eng. 2020;48:437–46. https://doi.org/10.1007/s10439-019-02361-7.

61. Freiser ME, Ghodadra A, Hirsch BE, McCall AA. Evaluation of 3D printed temporal Bone models in preparation for middle cranial fossa surgery. Otol Neurotol. 2019;40:246–53. https://doi.org/10.1097/MAO.0000000000002073.

62. Alshehri SA, Singh SK, Mosahebi A, Kalaskar DM. The current progress and critical analysis of three-dimensional scanning and three-dimensional printing applications in breast surgery. BJS Open. 2021;5 https://doi.org/10.1093/bjsopen/zrab025.

63. Annino DJJR, Hansen EE, Sethi RK, Horne S, Rettig EM, Uppaluri R, Goguen LA. Accuracy and outcomes of virtual surgical planning and 3D-printed guides for osseous free flap reconstruction of mandibular osteoradionecrosis. Oral Oncol. 2022;135:106239. https://doi.org/10.1016/j.oraloncology.2022.106239.

64. Bateman MG, Durfee WK, Iles TL, Martin CM, Liao K, Erdman AG, Iaizzo PA. Cardiac patient-specific three-dimensional models as surgical planning tools. Surgery. 2020;167:259–63. https://doi.org/10.1016/j.surg.2018.11.022.

65. Abudayyeh I, Gordon B, Ansari MM, Jutzy K, Stoletniy L, Hilliard A. A practical guide to cardiovascular 3D printing in clinical practice: overview and examples. J Interv Cardiol. 2018;31:375–83. https://doi.org/10.1111/joic.12446.

66. Page MJ, McKenzie JE, Bossuyt PM, Boutron I, Hoffmann TC, Mulrow CD, Shamseer L, Tetzlaff JM, Akl EA, Brennan SE, et al. The PRISMA 2020 statement: an updated guideline for reporting systematic reviews. BMJ. 2021;372:n71. https://doi.org/10.1136/bmj.n71.

67. George E, Liacouras P, Rybicki FJ, Mitsouras D. Measuring and establishing the accuracy and reproducibility of 3D printed medical models. Radiographics. 2017;37:1424–50. https://doi.org/10.1148/rg.2017160165.

68. Samei E, Bakalyar D, Boedeker K.L, Brady S, Fan J, Leng S, Myers KJ, Popescu LM, Giraldo JCR, Ranallo F, et al. Performance Evaluation of Computed Tomography Systems: The Report of AAPM Task Group 233. American Association of Physicists in Medicine 2019; https://www.aapm.org/pubs/reports/RPT_233.pdf.

69. Ferraro JM, Falter J, Lee S, Watanabe K, Wu T-H, Kim D-G, Ko C-C, Tanaka E, Deguchi T. Accuracy of three-dimensional printed models derived from cone-beam computed tomography. Angle Orthod. 2022;92:722–7. https://doi.org/10.2319/021122-128.1.

70. Ogden KM, Aslan C, Ordway N, Diallo D, Tillapaugh-Fay G, Soman P. Factors affecting dimensional accuracy of 3-D printed anatomical structures derived from CT data. J Digit Imaging. 2015;28:654–63. https://doi.org/10.1007/s10278-015-9803-7.

71. Brouwers L, Teutelink A, van Tilborg FA, de Jongh MA, Lansink KW, Bemelman M. Validation study of 3D-printed anatomical models using 2 PLA printers for preoperative planning in trauma surgery, a human cadaver study. Eur J Trauma Emerg Surg. 2019;45:1013–20. https://doi.org/10.1007/s00068-018-0970-3.

72. van Eijnatten M, Rijkhorst E-J, Hofman M, Forouzanfar T, Wolff J. The accuracy of ultrashort echo time MRI sequences for medical additive manufacturing. Dentomaxillofac Radiol. 2016;45:20150424. https://doi.org/10.1259/dmfr.20150424.

73. van Eijnatten M, Berger FH, de Graaf P, Koivisto J, Forouzanfar T, Wolff J. Influence of CT parameters on STL model accuracy. Rapid Prototyp J. 2017;23:678–85. https://doi.org/10.1108/RPJ-07-2015-0092.

74. Probst FA, Burian E, Malenova Y, Lyutskanova P, Stumbaum MJ, Ritschl LM, Kronthaler S, Karampinos D, Probst M. Geometric accuracy of magnetic resonance imaging-derived virtual 3-dimensional bone surface models of the mandible in comparison to computed tomography and cone beam computed tomography: A porcine cadaver study. Clin Implant Dent Relat Res. 2021;23:779–88. https://doi.org/10.1111/cid.13033.

75. van Eijnatten M, Koivisto J, Karhu K, Forouzanfar T, Wolff J. The impact of manual threshold selection in medical additive manufacturing. Int J Comput Assist Radiol Surg. 2017;12:607–15. https://doi.org/10.1007/s11548-016-1490-4.

76. Wagner M, Werther T, Unger E, Kasprian G, Dovjak G, Dorfer C, Schned H, Steinbauer P, Goeral K, Olischar M, et al. Development of a 3D printed patient-specific neonatal brain simulation model using multimodality imaging for perioperative management. Pediatr Res. 2022;91:64–9. https://doi.org/10.1038/s41390-021-01421-w.

77. Zhang C, Bruggink R, Baan F, Bronkhorst E, Maal T, He H, Ongkosuwito EM. A new segmentation algorithm for measuring CBCT images of nasal airway: a pilot study. PeerJ. 2019;7:e6246. https://doi.org/10.7717/peerj.6246.

78. Fogarasi M, Coburn JC, Ripley B. Algorithms used in medical image segmentation for 3D printing and how to understand and quantify their performance. 3D Print Med. 2022;8:18. https://doi.org/10.1186/s41205-022-00145-9.

79. Asmaria T, Annur D, Utomo MS, Sari AK, Malau DP, Prabowo Y, Rahyussalim AJ, Amal MI. Validation of 3D models using template matching for implant planning. 2019 16th International Conference on Quality in Research, QIR 2019 - International Symposium on Electrical and Computer Engineering. Padang: IEEE; 2019. p. 1–4. https://doi.org/10.1109/QIR.2019.8898275.

80. Allan A, Kealley C, Squelch A, Wong YH, Yeong CH, Sun Z. Patient-specific 3D printed model of biliary ducts with congenital cyst. Quant Imaging Med Surg. 2019;9:86–93. https://doi.org/10.21037/qims.2018.12.01.

81. Ho D, Squelch A, Sun Z. Modelling of aortic aneurysm and aortic dissection through 3D printing. J Med Radiat Sci. 2017;64:10–7. https://doi.org/10.1002/jmrs.212.

82. Edwards J, Rogers T. The accuracy and applicability of 3D modeling and printing blunt force cranial injuries. J Forensic Sci. 2018;63:683–91. https://doi.org/10.1111/1556-4029.13627.

83. Brown GB, Currier GF, Kadioglu O, Kierl JP. Accuracy of 3-dimensional printed dental models reconstructed from digital intraoral impressions. Am J Orthod Dentofacial Orthop. 2018;154:733–9. https://doi.org/10.1016/j.ajodo.2018.06.009.

84. de Alcântara Leite dos Reis D, Gouveia BLR, Júnior JCR, de Assis Neto AC. Comparative assessment of anatomical details of thoracic limb bones of a horse to that of models produced via scanning and 3D printing. 3D Print Med. 2019;5:13. https://doi.org/10.1186/s41205-019-0050-2.

85. Budzik G, Woźniak J, Paszkiewicz A, Przeszłowski Ł, Dziubek T, Dębski M. Methodology for the quality control process of additive manufacturing products made of polymer materials. Materials (Basel). 2021;14 https://doi.org/10.3390/ma14092202.

86. Gillett D, Bashari W, Senanayake R, Marsden D, Koulouri O, MacFarlane J, van der Meulen M, Powlson AS, Mendichovszky IA, Cheow H, et al. Methods of 3D printing models of pituitary tumors. 3D Print Med. 2021;7:24. https://doi.org/10.1186/s41205-021-00118-4.

87. Jaber ST, Hajeer MY, Khattab TZ, Mahaini L. Evaluation of the fused deposition modeling and the digital light processing techniques in terms of dimensional accuracy of printing dental models used for the fabrication of clear aligners. Clin Exp Dent Res. 2021;7:591–600. https://doi.org/10.1002/cre2.366.

88. Johansson C, Dibes J, Rodriguez LEL, Papia E. Accuracy of 3D printed polymers intended for models and surgical guides printed with two different 3D printers. Dent Mater J. 2021;40:339–47. https://doi.org/10.4012/dmj.2020-039.

89. Kim JH, Pinhata-Baptista OH, Ayres AP, Da Silva R, Lima JF, Urbano GS, et al. Accuracy Comparison among 3D-Printing Technologies to Produce Dental Models. Appl Sci (Switzerland). 2022;12 https://doi.org/10.3390/app12178425.

90. Kitsakis K, Alabey P, Kechagias J, Vaxevanidis N, eds. A Study of the dimensional accuracy obtained by low cost 3D printing for possible application in medicine. IOP Conference Series: Materials Science and Engineering; 2016. https://doi.org/10.1088/1757-899X/161/1/012025.

91. Lee S, Squelch A, Sun Z. Quantitative assessment of 3D printed model accuracy in delineating congenital heart disease. Biomolecules. 2021;11 https://doi.org/10.3390/biom11020270.

92. Manmadhachary A, Siva Rama Krishana L, Saxena KK. Quantification of the accuracy of additive manufactured (3D printed) medical models. Int J Interact Des Manuf. 2022; https://doi.org/10.1007/s12008-022-00949-3.

93. Olejník P, Nosal M, Havran T, Furdova A, Cizmar M, Slabej M, Thurzo A, Vitovic P, Klvac M, Acel T, et al. Utilisation of three-dimensional printed heart models for operative planning of complex congenital heart defects. Kardiol Pol. 2017;75:495–501. https://doi.org/10.5603/KP.a2017.0033.

94. Perens G, Chyu J, McHenry K, Yoshida T, Finn JP. Three-dimensional congenital heart models created with free software and a desktop printer: assessment of accuracy, technical aspects, and clinical use. World J Pediatr Congenit Heart Surg. 2020;11:797–801. https://doi.org/10.1177/2150135120952072.

95. Perica E, Sun Z. Patient-specific three-dimensional printing for presurgical planning in hepatocellular carcinoma treatment. Quant Imaging Med Surg. 2017;7:668–77. https://doi.org/10.21037/qims.2017.11.02.

96. Ravi P, Chepelev L, Lawera N, Haque KMA, Chen VCP, Ali A, Rybicki FJ. A systematic evaluation of medical 3D printing accuracy of multi-pathological anatomical models for surgical planning manufactured in elastic and rigid material using desktop inverted vat photopolymerization. Med Phys. 2021;48:3223–33. https://doi.org/10.1002/mp.14850.

97. Ravi P, Chepelev LL, Stichweh GV, Jones BS, Rybicki FJ. Medical 3D printing dimensional accuracy for multi-pathological anatomical models 3D printed using material extrusion. J Digit Imaging. 2022;35:613–22. https://doi.org/10.1007/s10278-022-00614-x.

98. Rebong RE, Stewart KT, Utreja A, Ghoneima AA. Accuracy of three-dimensional dental resin models created by fused deposition modeling, stereolithography, and Polyjet prototype technologies: A comparative study. Angle Orthod. 2018;88:363–9. https://doi.org/10.2319/071117-460.1.

99. Suryajaya W, Ismah N, Purbiati M. Accuracy of digital dental models and three-dimensional printed dental models in linear measurements and Bolton analysis. F1000Res. 2021;10:10.12688/f1000research.31865.1.

100. Unkovskiy A, Spintzyk S, Axmann D, Engel E-M, Weber H, Huettig F. Additive manufacturing: A comparative analysis of dimensional accuracy and skin texture reproduction of auricular prostheses replicas. J Prosthodont. 2019;28:e460–8. https://doi.org/10.1111/jopr.12681.

101. Zeller A-N, Neuhaus M-T, Fresenborg S, Zimmerer RM, Jehn P, Spalthoff S, Gellrich N-C, Dittmann JA. Accurate and cost-effective mandibular biomodels: a standardized evaluation of 3D-printing via fused layer deposition modeling on soluble support structures. J Stomatol Oral Maxillofac Surg. 2021;122:355–60. https://doi.org/10.1016/j.jormas.2020.09.018.

102. Ahmad MN, Tarmeze AA, Abdul Rasib AH. Capability of 3d printing technology in producing molar teeth prototype. Int J Eng Appl. 2020;8:64–70. https://doi.org/10.15866/irea.v8i2.17949.

103. Akyalcin S, Rutkowski P, Arrigo M, Trotman CA, Kasper FK. Evaluation of current additive manufacturing systems for orthodontic 3-dimensional printing. Am J Orthod Dentofacial Orthop. 2021;160:594–602. https://doi.org/10.1016/j.ajodo.2020.12.022.

104. Anadioti E, Kane B, Zhang Y, Bergler M, Mante F, Blatz MB. Accuracy of dental and industrial 3D printers. J Prosthodont. 2022;31:30–7. https://doi.org/10.1111/jopr.13470.

105. Bud ES, Bocanet VI, Muntean MH, Vlasa A, Bucur SM, Păcurar M, et al. Accuracy of three-dimensional (3D) printed dental digital models generated with three types of resin polymers by extra-Oral optical scanning. J Clin Med. 2021;10 https://doi.org/10.3390/jcm10091908.

106. Buhrer Samra AP, Pomini MC, Granville F, Zavolski A, de Oliveira FB, Dias AH. Three-dimensional printed models versus conventional stone models: an accuracy analysis. Braz J Oral Sci. 2020;19:1–9. https://doi.org/10.20396/bjos.v19i0.8659937.

107. Emir F, Ayyildiz S. Accuracy evaluation of complete-arch models manufactured by three different 3D printing technologies: a three-dimensional analysis. J Prosthodont Res. 2021;65:365–70. https://doi.org/10.2186/jpr.JPOR_2019_579.

108. Ferraiuoli P, Taylor JC, Martin E, Fenner JW, Narracott AJ. The accuracy of 3D optical reconstruction and additive manufacturing processes in reproducing detailed subject-specific anatomy. J Imaging. 2017;3 https://doi.org/10.3390/jimaging3040045.

109. Jeong Y-G, Lee W-S, Lee K-B. Accuracy evaluation of dental models manufactured by CAD/CAM milling method and 3D printing method. J Adv Prosthodont. 2018;10:245–51. https://doi.org/10.4047/jap.2018.10.3.245.

110. Yoo S-Y, Kim S-K, Heo S-J, Koak J-Y, Kim J-G. Dimensional accuracy of dental models for three-unit prostheses fabricated by various 3D printing technologies. Materials (Basel). 2021;14 https://doi.org/10.3390/ma14061550.

111. Alexandru-Victor B, Cristina G, Sorana B, Marius M, Diana D, Radu-Septimiu C. Three-dimensional accuracy evaluation of two additive manufacturing processes in the production of dental models. Key Engineering Materials; 2017. p. 119–25.

112. Bertolini M, Rossoni M, Colombo G. Operative workflow from CT to 3D printing of the heart: opportunities and challenges. Bioengineering (Basel). 2021;8 https://doi.org/10.3390/bioengineering8100130.

113. Czajkowska M, Walejewska E, Zadrożny Ł, Wieczorek M, Święszkowski W, Wagner L, et al. Comparison of dental stone models and their 3D printed acrylic replicas for the accuracy and mechanical properties. Materials (Basel). 2020;13 https://doi.org/10.3390/ma13184066.

114. Dietrich CA, Ender A, Baumgartner S, Mehl A. A validation study of reconstructed rapid prototyping models produced by two technologies. Angle Orthod. 2017;87:782–7. https://doi.org/10.2319/01091-727.1.

115. Dong T, Wang X, Xia L, Yuan L, Ye N, Fang B. Accuracy of different tooth surfaces on 3D printed dental models: orthodontic perspective. BMC Oral Health. 2020;20:340. https://doi.org/10.1186/s12903-020-01338-6.

116. Fasel J, Malis DD, Wiederer C, Hagenbuch N. 3D printing of anatomical models for surgeons: an investigation on repeatability. Int J Interact Des Manuf. 2018;12:621–7. https://doi.org/10.1007/s12008-018-0478-4.

117. Greco GB, Popi D, Di Stefano DA. Accuracy of 3-dimensional printing of dental casts: A proposal for quality standardization. J Prosthet Dent. 2022;127:899–910. https://doi.org/10.1016/j.prosdent.2020.09.045.

118. Hatz CR, Msallem B, Aghlmandi S, Brantner P, Thieringer FM. Can an entry-level 3D printer create high-quality anatomical models? Accuracy assessment of mandibular models printed by a desktop 3D printer and a professional device. Int J Oral Maxillofac Surg. 2020;49:143–8. https://doi.org/10.1016/j.ijom.2019.03.962.

119. Im C-H, Park J-M, Kim J-H, Kang Y-J, Kim J-H. Assessment of compatibility between various intraoral scanners and 3d printers through an accuracy analysis of 3d printed models. Materials (Basel). 2020;13 https://doi.org/10.3390/ma13194419.

120. Jin G, Shin S-H, Shim J-S, Lee K-W, Kim J-E. Accuracy of 3D printed models and implant-analog positions according to the implant-analog-holder offset, inner structure, and printing layer thickness: an in-vitro study. J Dent. 2022;125:104268. https://doi.org/10.1016/j.jdent.2022.104268.

121. Johnson A, Jani G, Carew R, Pandey A. Assessment of the accuracy of 3D printed teeth by various 3D printers in forensic odontology. Forensic Sci Int. 2021;328 https://doi.org/10.1016/j.forsciint.2021.111044.

122. Msallem B, Sharma N, Cao S, Halbeisen FS, Zeilhofer H-F, Thieringer FM. Evaluation of the dimensional accuracy of 3D-printed anatomical mandibular models using FFF, SLA, SLS, MJ, and BJ printing technology. J Clin Med. 2020;9 https://doi.org/10.3390/jcm9030817.

123. Shin S-H, Kwon J-S, Shim J-S, Kim J-E. Evaluating the three-dimensional printing accuracy of partial-arch models according to Outer Wall thickness: an in vitro study. Materials (Basel). 2021;14 https://doi.org/10.3390/ma14226734.

124. Rungrojwittayakul O, Kan JY, Shiozaki K, Swamidass RS, Goodacre BJ, Goodacre CJ, Lozada JL. Accuracy of 3D printed models created by two Technologies of Printers with different designs of Model Base. J Prosthodont. 2020;29:124–8. https://doi.org/10.1111/jopr.13107.

125. Sokolowski AA, Kammerhofer J, Madreiter-Sokolowski CT, Payer M, Koller M, Jakse N, Wegscheider WA. Accuracy assessment of 3D-printed tooth replicas. Int J Comput Dent. 2019;22:321–9.

126. Tóth T, Varga P, Štefanovič B, Bednarčíková L, Schnitzer M, Hudák R, Živčák J. Accuracy verification of an anatomical model manufactured using low-cost additive production. Appl Sci (Switzerland). 2021;11:1–19. https://doi.org/10.3390/app11020594.

127. Turek P, Budzik G. Estimating the accuracy of mandible anatomical models manufactured using material extrusion methods. Polymers (Basel). 2021;13 https://doi.org/10.3390/polym13142271.

128. Zhang Z-C, Li P-L, Chu F-T, Shen G. Influence of the three-dimensional printing technique and printing layer thickness on model accuracy. J Orofac Orthop. 2019;80:194–204. https://doi.org/10.1007/s00056-019-00180-y.

129. Bati AH, Guler E, Ozer MA, Govsa F, Erozkan K, Vatansever S, Ersin MS, Elmas ZN, Harman M. Surgical planning with patient-specific three-dimensional printed pancreaticobiliary disease models - cross-sectional study. Int J Surg. 2020;80:175–83. https://doi.org/10.1016/j.ijsu.2020.06.017.

130. Birbara NS, Otton JM, Pather N. 3D modelling and printing technology to produce patient-specific 3D models. Heart Lung Circ. 2019;28:302–13. https://doi.org/10.1016/j.hlc.2017.10.017.

131. Ishida Y, Miura D, Miyasaka T, Shinya A. Dimensional accuracy of dental casting patterns fabricated using consumer 3D printers. Polymers (Basel). 2020;12 https://doi.org/10.3390/polym12102244.

132. Kamio T, Hayashi K, Onda T, Takaki T, Shibahara T, Yakushiji T, Shibui T, Kato H. Utilizing a low-cost desktop 3D printer to develop a "one-stop 3D printing lab" for oral and maxillofacial surgery and dentistry fields. 3D Print Med. 2018;4:6. https://doi.org/10.1186/s41205-018-0028-5.

133. Legocki AT, Duffy-Peter A, Scott AR. Benefits and limitations of entry-level 3-dimensional printing of maxillofacial skeletal models. JAMA Otolaryngol Head Neck Surg. 2017;143:389–94. https://doi.org/10.1001/jamaoto.2016.3673.

134. Leng S, McGee K, Morris J, Alexander A, Kuhlmann J, Vrieze T, McCollough CH, Matsumoto J. Anatomic modeling using 3D printing: quality assurance and optimization. 3D Print Med. 2017;3:6. https://doi.org/10.1186/s41205-017-0014-3.

135. Liang X, Liao W, Cai H, Jiang S, Chen S. 3D-printed artificial teeth: accuracy and application in root canal therapy. J Biomed Nanotechnol. 2018;14:1477–85. https://doi.org/10.1166/jbn.2018.2599.

136. Mangano FG, Admakin O, Bonacina M, Biaggini F, Farronato D, Lerner H. Accuracy of 6 desktop 3D printers in dentistry: A comparative in vitro study. Eur J Prosthodont Restor Dent. 2020;28:75–85. https://doi.org/10.1922/EJPRD_2050Mangano11.

137. Rynio P, Wojtuń M, Wójcik Ł, Kawa M, Falkowski A, Gutowski P, Kazimierczak A. The accuracy and reliability of 3D printed aortic templates: a comprehensive three-dimensional analysis. Quant Imaging Med Surg. 2022;12:1385–96. https://doi.org/10.21037/qims-21-529.

138. Salmi M, Paloheimo K-S, Tuomi J, Wolff J, Mäkitie A. Accuracy of medical models made by additive manufacturing (rapid manufacturing). J Craniomaxillofac Surg. 2013;41:603–9. https://doi.org/10.1016/j.jcms.2012.11.041.

139. Turek P, Budzik G, Przeszłowski Ł. Assessing the radiological density and accuracy of mandible polymer anatomical structures manufactured using 3D printing technologies. Polymers (Basel). 2020;12 https://doi.org/10.3390/polym12112444.

140. Turek P, Filip D, Przeszłowski Ł, Łazorko A, Budzik G, Snela S, et al. Manufacturing polymer model of anatomical structures with increased accuracy using cax and am systems for planning orthopedic procedures. Polymers (Basel). 2022;14 https://doi.org/10.3390/polym14112236.

141. Witowski J, Wake N, Grochowska A, Sun Z, Budzyński A, Major P, Popiela TJ, Pędziwiatr M. Investigating accuracy of 3D printed liver models with computed tomography. Quant Imaging Med Surg. 2019;9:43–52. https://doi.org/10.21037/qims.2018.09.16.

142. Aristotle S, Patil S, Jayakumar S. Dimensional accuracy of medical models of the skull produced by three-dimensional printing technology by advanced morphometric analysis. J Anat Soc India. 2022;71:186–90. https://doi.org/10.4103/jasi.jasi_202_21.

143. Cai T, Rybicki FJ, Giannopoulos AA, Schultz K, Kumamaru KK, Liacouras P, Demehri S, Shu Small KM, Mitsouras D. The residual STL volume as a metric to evaluate accuracy and reproducibility of anatomic models for 3D printing: application in the validation of 3D-printable models of maxillofacial bone from reduced radiation dose CT images. 3D Print Med. 2015;1:2. https://doi.org/10.1186/s41205-015-0003-3.

144. Kim GY, Li J, Moon HS, Oh KC. Accuracy of additively manufactured dental casts compared with that of virtual scan data obtained with an intraoral scanner: an in vitro study. Appl Sci (Switzerland). 2022;12 https://doi.org/10.3390/app12094348.

145. Luzon JA, Andersen BT, Stimec BV, Fasel JHD, Bakka AO, Kazaryan AM, Ignjatovic D. Implementation of 3D printed superior mesenteric vascular models for surgical planning and/or navigation in right colectomy with extended D3 mesenterectomy: comparison of virtual and physical models to the anatomy found at surgery. Surg Endosc. 2019;33:567–75. https://doi.org/10.1007/s00464-018-6332-8.

146. Sun Z, Squelch A. Patient-specific 3D printed models of aortic aneurysm and aortic dissection. J Med Imaging Health Info. 2017;7:886–9. https://doi.org/10.1166/jmihi.2017.2093.

147. Kodym O, Španěl M, Herout A. Segmentation of Defective Skulls from CT Data for Tissue Modelling. Lecture Notes in Computer Science (including subseries Lecture Notes in Artificial Intelligence and Lecture Notes in Bioinformatics); 2021. p. 19–28.

148. Lo Giudice A, Quinzi V, Ronsivalle V, Farronato M, Nicotra C, Indelicato F, et al. Evaluation of imaging software accuracy for 3-dimensional analysis of the mandibular condyle. A comparative study using a surface-to-surface matching technique. Int J Environ Res Public Health. 2020;17 https://doi.org/10.3390/ijerph17134789.

149. Minnema J, van Eijnatten M, Kouw W, Diblen F, Mendrik A, Wolff J. CT image segmentation of bone for medical additive manufacturing using a convolutional neural network. Comput Biol Med. 2018;103:130–9. https://doi.org/10.1016/j.compbiomed.2018.10.012.

150. Matsiushevich K, Belvedere C, Leardini A, Durante S. Quantitative comparison of freeware software for bone mesh from DICOM files. J Biomech. 2019;84:247–51. https://doi.org/10.1016/j.jbiomech.2018.12.031.

151. Bertolini M, Luraghi G, Belicchi I, Migliavacca F, Colombo G. Evaluation of segmentation accuracy and its impact on patient-specific CFD analysis. Int J Interact Des Manuf. 2022;16:545–56. https://doi.org/10.1007/s12008-021-00802-z.

152. Aly P, Mohsen C. Comparison of the accuracy of three-dimensional printed casts, digital, and conventional casts: an in vitro study. Eur J Dent. 2020;14:189–93. https://doi.org/10.1055/s-0040-1705243.

153. Carew RM, Morgan RM, Rando C. A preliminary investigation into the accuracy of 3D modeling and 3D printing in forensic anthropology evidence reconstruction. J Forensic Sci. 2019;64:342–52. https://doi.org/10.1111/1556-4029.13917.

154. Mowers KL, Fullerton JB, Hicks D, Singh GK, Johnson MC, Anwar S. 3D echocardiography provides highly accurate 3D printed models in congenital heart disease. Pediatr Cardiol. 2021;42:131–41. https://doi.org/10.1007/s00246-020-02462-4.

155. Salazar DA, Cramer J, Markin NW, Hunt NH, Linke G, Siebler J, et al. Comparison of 3D printed anatomical model qualities in acetabular fracture representation. Ann Transl Med. 2022;10(391) https://doi.org/10.21037/atm-21-5069.

156. van Eijnatten M, Wolff J, Pauwels R, Karhu K, Hietanen A, der Sarkissian H, Koivisto JH. Influence of head positioning during cone-beam CT imaging on the accuracy of virtual 3D models. Dentomaxillofac Radiol. 2022;51:20220104. https://doi.org/10.1259/dmfr.20220104.

157. Ionita CN, Mokin M, Varble N, Bednarek DR, Xiang J, Snyder KV, Siddiqui AH, Levy EI, Meng H, Rudin S. Challenges and limitations of patient-specific vascular phantom fabrication using 3D Polyjet printing. Proc SPIE Int Soc Opt Eng. 2014;9038:90380M. https://doi.org/10.1117/12.2042266.

158. Eley KA, Watt-Smith SR, Golding SJ. "black Bone" MRI: a novel imaging technique for 3D printing. Dentomaxillofac Radiol. 2017;46:20160407. https://doi.org/10.1259/dmfr.20160407.

159. Hesham NM, Kandil H, Dakhli II. Evaluation of dimensional accuracy of 3D printed mandibular model using two different additive manufacturing techniques based on ultralow dose multislice computed tomography scan data: A diagnostic accuracy study. J Int Oral Health. 2022;14:86–93. https://doi.org/10.4103/jioh.jioh_210_21.

160. Igai F, Junior W-S, Iegami C-M, Neto P-T. Assessment of different types of intra oral scanners and 3D printers on the accuracy of printed models: an in vitro study. J Clin Exp Dent. 2021;13:e1174–81. https://doi.org/10.4317/jced.58765.

161. Macatangay I, Malipot J, Lopez A, Mabulay R, Magpantay R, Malecdan LS, Malingan J, Malolos G, Mamaril P, Mananghaya A, et al. Dimensional accuracy of 3d-printed models of the right first metacarpal bones of cadavers. Acta Medica Philippina. 2020;54:454–61. https://doi.org/10.47895/AMP.V54I5.2212.

162. McMenamin PG, Quayle MR, McHenry CR, Adams JW. The production of anatomical teaching resources using three-dimensional (3D) printing technology. Anat Sci Educ. 2014;7:479–86. https://doi.org/10.1002/ase.1475.

163. Mejia S, Stewart N, Miller A, Savicky R, Monarski C, Moore GE, Keith D. Accuracy of external measurements of 3-dimensional (3D) printed biomodels of the canine radius used in an in-hospital setting. Can J Vet Res. 2019;83:181–6.

164. Petropolis C, Kozan D, Sigurdson L. Accuracy of medical models made by consumer-grade fused deposition modelling printers. Plast Surg (Oakv). 2015;23:91–4. https://doi.org/10.4172/plastic-surgery.1000912.

165. Silva DN, Gerhardt de Oliveira M, Meurer E, Meurer MI, Da Lopes Silva JV, Santa-Bárbara A. Dimensional error in selective laser sintering and 3D-printing of models for craniomaxillary anatomy reconstruction. J Craniofac Surg. 2008;36:443–9. https://doi.org/10.1016/j.jcms.2008.04.003.

166. Yousefi F, Shokri A, Farhadian M, Vafaei F, Forutan F. Accuracy of maxillofacial prototypes fabricated by different 3-dimensional printing technologies using multi-slice and cone-beam computed tomography. Imaging Sci Dent. 2021;51:41–7. https://doi.org/10.5624/isd.20200175.

167. Lebowitz C, Massaglia J, Hoffman C, Lucenti L, Dheer S, Rivlin M, Beredjiklian PK. The accuracy of 3D printed carpal bones generated from cadaveric specimens. Arch Bone Jt Surg. 2021;9:432–8. https://doi.org/10.22038/abjs.2020.50236.2495.

168. Boursier J-F, Fournet A, Bassanino J, Manassero M, Bedu A-S, Leperlier D. Reproducibility, accuracy and effect of autoclave sterilization on a thermoplastic three-dimensional model printed by a desktop fused deposition modelling three-dimensional printer. Vet Comp Orthop Traumatol. 2018;31:422–30. https://doi.org/10.1055/s-0038-1668113.

169. Cantré D, Langner S, Kaule S, Siewert S, Schmitz K-P, Kemmling A, Weber M-A. Three-dimensional imaging and three-dimensional printing for plastic preparation of medical interventions. Radiologe. 2020;60:70–9. https://doi.org/10.1007/s00117-020-00739-6.

170. Hedelin H, Swinkels CS, Laine T, Mack K, Lagerstrand K. Using a 3D printed model as a preoperative tool for pelvic triple osteotomy in children: proof of concept and evaluation of geometric accuracy. J Am Acad Orthop Surg Glob Res Rev. 2019;3:e074. https://doi.org/10.5435/JAAOSGlobal-D-18-00074.

171. Hsieh T-Y, Cervenka B, Dedhia R, Strong EB, Steele T. Assessment of a patient-specific, 3-dimensionally printed endoscopic sinus and Skull Base surgical model. JAMA Otolaryngol Head Neck Surg. 2018;144:574–9. https://doi.org/10.1001/jamaoto.2018.0473.

172. Kaschwich M, Horn M, Matthiensen S, Stahlberg E, Behrendt C-A, Matysiak F, Bouchagiar J, Dell A, Ellebrecht D, Bayer A, et al. Accuracy evaluation of patient-specific 3D-printed aortic anatomy. Ann Anat. 2021;234:151629. https://doi.org/10.1016/j.aanat.2020.151629.

173. Lau I, Wong YH, Yeong CH, Abdul Aziz YF, Md Sari NA, Hashim SA, Sun Z. Quantitative and qualitative comparison of low- and high-cost 3D-printed heart models. Quant Imaging Med Surg. 2019;9:107–14. https://doi.org/10.21037/qims.2019.01.02.

174. Maier P, Silvestro E, Goldfarb SB, Piccione J, Phinizy PA, Andronikou S. Three-dimensional printed realistic pediatric static and dynamic airway models for bronchoscopy and foreign body removal training. Pediatr Pulmonol. 2021;56:2654–9. https://doi.org/10.1002/ppul.25516.

175. Michiels C, Jambon E, Bernhard JC. Measurement of the accuracy of 3D-printed medical models to be used for robot-assisted partial nephrectomy. AJR Am J Roentgenol. 2019;213:626–31. https://doi.org/10.2214/AJR.18.21048.

176. Aluwee S, Bin SAZ, Zhou X, Kato H, Makino H, Muramatsu C, Hara T, Matsuo M, Fujita H. Evaluation of pre-surgical models for uterine surgery by use of three-dimensional printing and mold casting. Radiol Phys Technol. 2017;10:279–85. https://doi.org/10.1007/s12194-017-0397-2.

177. Shibata E, Takao H, Amemiya S, Ohtomo K. 3D-printed visceral aneurysm models based on CT data for simulations of endovascular embolization: evaluation of size and shape accuracy. AJR Am J Roentgenol. 2017;209:243–7. https://doi.org/10.2214/AJR.16.17694.

178. Zou Y, HAN Q, Weng X, Yang Y, Zhang K, Yang K, et al. The precision and reliability evaluation of 3-dimensional printed damaged bone and prosthesis models by stereo lithography appearance. Medicine (United States). 2018;97 https://doi.org/10.1097/MD.0000000000009797.

179. Anderson JR, Thompson WL, Alkattan AK, Diaz O, Klucznik R, Zhang YJ, Britz GW, Grossman RG, Karmonik C. Three-dimensional printing of anatomically accurate, patient specific intracranial aneurysm models. J Neurointerv Surg. 2016;8:517–20. https://doi.org/10.1136/neurintsurg-2015-011686.

180. Cohen J, Reyes SA. Creation of a 3D printed temporal bone model from clinical CT data. Am J Otolaryngol - Head Neck Med Surg. 2015;36:619–24. https://doi.org/10.1016/j.amjoto.2015.02.012.

181. Faletti R, Gatti M, Cosentino A, Bergamasco L, Cura Stura E, Garabello D, Pennisi G, Salizzoni S, Veglia S, Ottavio D, et al. 3D printing of the aortic annulus based on cardiovascular computed tomography: preliminary experience in pre-procedural planning for aortic valve sizing. J Cardiovasc Comput Tomogr. 2018;12:391–7. https://doi.org/10.1016/j.jcct.2018.05.016.

182. Kappanayil M, Koneti NR, Kannan RR, Kottayil BP, Kumar K. Three-dimensional-printed cardiac prototypes aid surgical decision-making and preoperative planning in selected cases of complex congenital heart diseases: early experience and proof of concept in a resource-limited environment. Ann Pediatr Cardiol. 2017;10:117–25. https://doi.org/10.4103/apc.APC_149_16.

183. Larguier L, Hespel AM, Jamet N, Mercier E, Jouan D, Jardel N, Larrat S. Accuracy and precision of measurements performed on three-dimensional printed pelvises when compared to computed tomography measurements. J Vet Sci. 2019;20:e22. https://doi.org/10.4142/jvs.2019.20.e22.

184. Ma C-Y, Wang T-H, Yu W-C, Shih Y-C, Lin C-H, Perng C-K, Ma H, Wang S-J, Chen W-M, Chen C-E. Accuracy of the application of 3-dimensional printing models in orbital blowout fractures-A preliminary study. Ann Plast Surg. 2022;88:S33–8. https://doi.org/10.1097/SAP.0000000000 003166.

185. Muraru D, Veronesi F, Maddalozzo A, Dequal D, Frajhof L, Rabischoffsky A, Iliceto S, Badano LP. 3D printing of normal and pathologic tricuspid valves from transthoracic 3D echocardiography data sets. Eur Heart J Cardiovasc Imaging. 2017;18:802–8. https://doi.org/10.1093/ehjci/jew215.

186. Naftulin JS, Kimchi EY, Cash SS. Streamlined, inexpensive 3D printing of the brain and skull. PLoS One. 2015;10 https://doi.org/10.1371/journal.pone.0136198.

187. Scanlan AB, Nguyen AV, Ilina A, Lasso A, Cripe L, Jegatheeswaran A, Silvestro E, McGowan FX, Mascio CE, Fuller S, et al. Comparison of 3D echocardiogram-derived 3D printed valve models to molded models for simulated repair of pediatric atrioventricular valves. Pediatr Cardiol. 2018;39:538–47. https://doi.org/10.1007/s00246-017-1785-4.

188. Valverde I, Gomez G, Coserria JF, Suarez-Mejias C, Uribe S, Sotelo J, Velasco MN, Santos De Soto J, Hosseinpour A-R, Gomez-Cia T. 3D printed models for planning endovascular stenting in transverse aortic arch hypoplasia. Catheter Cardiovasc Interv. 2015;85:1006–12. https://doi.org/10.1002/ccd.25810.

189. Wang L, Ye X, Hao Q, Ma L, Chen X, Wang H, Zhao Y. Three-dimensional intracranial middle cerebral artery aneurysm models for aneurysm surgery and training. J Clin Neurosci. 2018;50:77–82. https://doi.org/10.1016/j.jocn.2018.01.074.

190. Wu A-M, Shao Z-X, Wang J-S, Yang X-D, Weng W-Q, Wang X-Y, Xu H-Z, Chi Y-L, Lin Z-K. The accuracy of a method for printing three-dimensional spinal models. PLoS One. 2015;10:e0124291. https://doi.org/10.1371/journal.pone.0124291.

191. Kociński M, Materka A, Elgalal M, Majos A. On accuracy of personalized 3D-printed MRI-based models of brain arteries. International Conference on Systems, Signals, and Image Processing. IEEE: Poznan: 2017. p. 1–5. https://doi.org/10.1109/IWSSIP.2017.7965601.

192. Shepard LM, Sommer KN, Angel E, Iyer V, Wilson MF, Rybicki FJ, et al. Initial evaluation of three-dimensionally printed patient-specific coronary phantoms for CT-FFR software validation. J Med Imaging. 2019;6 https://doi.org/10.1117/1.JMI.6.2.021603.

193. Takao H, Amemiya S, Shibata E, Ohtomo K. 3D printing of preoperative simulation models of a splenic artery aneurysm: precision and accuracy. Acad Radiol. 2017;24:650–3. https://doi.org/10.1016/j.acra.2016.12.015.

194. Waran V, Menon R, Pancharatnam D, Rathinam AK, Balakrishnan YK, Tung TS, Raman R, Prepageran N, Chandran H, Rahman ZAA. The creation and verification of cranial models using three-dimensional rapid prototyping technology in field of transnasal sphenoid endoscopy. Am J Rhinol Allergy. 2012;26:e132–6. https://doi.org/10.2500/ajra.2012.26.3808.

195. Choi J-W, Ahn J-J, Son K, Huh J-B. Three-dimensional evaluation on accuracy of conventional and milled gypsum models and 3D printed photopolymer models. Materials (Basel). 2019;12 https://doi.org/10.3390/ma12213499.

196. Dorweiler B, Baqué PE, Chaban R, Ghazy A, Salem O. Quality control in 3D printing: accuracy analysis of 3D-printed models of patient-specific anatomy. Materials (Basel). 2021;14 https://doi.org/10.3390/ma140 41021.

197. Jin S-J, Jeong I-D, Kim J-H, Kim W-C. Accuracy (trueness and precision) of dental models fabricated using additive manufacturing methods. Int J Comput Dent. 2018;21:107–13.

198. Jin S-J, Kim D-Y, Kim J-H, Kim W-C. Accuracy of dental replica models using photopolymer materials in additive manufacturing: in vitro three-dimensional evaluation. J Prosthodont. 2019;28:e557–62. https://doi.org/10.1111/jopr.12928.

199. Bone TM, Mowry SE. Content validity of temporal Bone models printed via inexpensive methods and materials. Otology and Neurotology; 2016. p. 1183–8.

200. Darr C, Finis F, Wiesenfarth M, Giganti F, Tschirdewahn S, Krafft U, Kesch C, Bonekamp D, Forsting M, Wetter A, et al. Three-dimensional magnetic resonance imaging-based printed models of prostate anatomy and targeted biopsy-proven index tumor to facilitate patient-tailored radical prostatectomy-A feasibility study. Eur Urol Oncol. 2022;5:357–61. https://doi.org/10.1016/j.euo.2020.08.004.

201. Morón-Conejo B, López-Vilagran J, Cáceres D, Berrendero S, Pradíes G. Accuracy of five different 3D printing workflows for dental models comparing industrial and dental desktop printers. Clin Oral Investig. 2022; https://doi.org/10.1007/s00784-022-04809-y.

202. Miyazaki T, Hotta Y, Kunii J, Kuriyama S, Tamaki Y. A review of dental CAD/CAM: current status and future perspectives from 20 years of experience. Dent Mater J. 2009;28:44–56. https://doi.org/10.4012/dmj.28.44.

203. Rekow ED. Digital dentistry: The new state of the art - is it disruptive or destructive? Dent Mater. 2020;36:9–24. https://doi.org/10.1016/j.dental.2019.08.103.

204. Lin L, Fang Y, Liao Y, Chen G, Gao C, Zhu P. 3D printing and digital processing techniques in dentistry: A review of literature. Adv Eng Mater. 2019;21 https://doi.org/10.1002/adem.201801013.

205. Zhang J, Su Y, Rao X, Pang H, Zhu H, Liu L, Chen L, Li D, He J, Peng J, et al. Additively manufactured polyether ether ketone (PEEK) skull implant as an alternative to titanium mesh in cranioplasty. Int J Bioprint. 2023;9:634. https://doi.org/10.18063/ijb.v9i1.634.

206. Uehara M, Takahashi J, Ikegami S, Kuraishi S, Futatsugi T, Oba H, Takizawa T, Munakata R, Koseki M, Kato H. How much surface registration accuracy is required using Ct-based navigation system in adolescent idiopathic scoliosis surgery? Clin Spine Surg. 2019;32:E166–70. https://doi.org/10.1097/BSD.0000000000000759.

207. Laitinen MK, Parry MC, Albergo JI, Grimer RJ, Jeys LM. Is computer navigation when used in the surgery of iliosacral pelvic bone tumours safer for the patient? Bone Joint J. 2017;99-B:261–6. https://doi.org/10.1302/0301-620X.99B2.BJJ-2016-0149.R2.

208. Cho HS, Oh JH, Han I, Kim H-S. The outcomes of navigation-assisted bone tumour surgery: minimum three-year follow-up. J Bone Joint Surg Br. 2012;94:1414–20. https://doi.org/10.1302/0301-620X.94B10.28638.

209. Witowski JS, Pędziwiatr M, Major P, Budzyński A. Cost-effective, personalized, 3D-printed liver model for preoperative planning before laparoscopic liver hemihepatectomy for colorectal cancer metastases. Int J Comput Assist Radiol Surg. 2017;12:2047–54. https://doi.org/10.1007/s11548-017-1527-3.

210. Odeh M, Levin D, Inziello J, Lobo Fenoglietto F, Mathur M, Hermsen J, Stubbs J, Ripley B. Methods for verification of 3D printed anatomic model accuracy using cardiac models as an example. 3D Print Med. 2019;5:6. https://doi.org/10.1186/s41205-019-0043-1.

Publisher's Note